PERFORMANCE MODELS FOR DISTRIBUTED-MEMORY HPC SYSTEMS AND DEEP NEURAL NETWORKS

A Thesis

Submitted to the Faculty

of

Purdue University

by

David Cardwell

In Partial Fulfillment of the

Requirements for the Degree

of

Master of Science

December 2019

Purdue University

Indianapolis, Indiana

THE PURDUE UNIVERSITY GRADUATE SCHOOL
STATEMENT OF THESIS APPROVAL

ACKNOWLEDGMENTS

I would like to thank Professor Song for his guidance in preparing this thesis.

TABLE OF CONTENTS

LIST OF TABLES

LIST OF FIGURES

ABSTRACT

Cardwell, David M.S., Purdue University, December 2019. Performance Models for Distributed-Memory HPC Systems And Deep Neural Networks. Major Professor: Fengguang Song.

Performance models are useful as mathematical models to reason about the behavior of different computer systems while running various applications. An additional purpose is predicting performance without having to run a given application on a target system. Models that simultaneously provide accurate results as well as insight in optimization techniques are difficult to develop since more accurate models tend to be more complex. Straightforward and precise models are of great interest for this reason.

In this thesis, we aim to provide two distinct performance models: one for distributed-memory high performance computing systems with network communication, and one for deep neural networks. Our main goal for the first model is insight and simplicity, while for the second we aim for accuracy in prediction. The first model is generalized for networked multi-core computer systems, while the second is specific to deep neural networks on a shared-memory system.

First, we enhance the well-known Roofline model with extensions to add communication awareness. To do so, we introduce the concept of communication arithmetic intensity, which is the network equivalent of operational intensity. In the second model, we use performance measurements from target systems to parameterize the model by the problem size. For both models, we performed an empirical analysis on several target systems with various algorithms and applications to verify the quality of the predictions.

With our communication-aware extended Roofline model, we improve on the original model by up to 100% on all three tested computer systems according to our MAPE-based comparision method. For the deep neural network model, we attain up to a 23.43% absolute prediction error.

To our knowledge, our communication-aware Roofline model is the first Roofline extension to consider communication, while our second model is the first model of deep neural networks that uses parameterization.

1. INTRODUCTION

Performance models are a key part of performance studies and are widely used in High Performance Computing to predict the runtime efficiency of running various applications on assorted computer systems. These models allow insight to be gained on how a program can be optimized or where bottlenecks exist on particular hardware configurations. This allows implementers to better determine how to increase the performance of their applications, whether optimizing the code itself or changing the hardware.

A core issue of performance modeling is the level of complexity of the model. Generally, more complex models allow for higher prediction accuracy, but this comes at the cost of the intuitiveness of the model. For example, if the level of abstraction is low, such as at the level of microarchitectural details such as out-of-order execution, the model can become difficult to reason about. On the other hand, a model that is high-level may provide intuition about performance bottlenecks but little efficacy in prediction. Models that manage to be simple and accurate are of interest since they solve both concerns. One such model is the Roofline model, which is both simple and widely-used.

Performance models are of particular interest in High Performance Computing, where speed of execution and optimization are core goals. Since these systems are distributed-memory and rely on networks, modeling the interconnect is important since it is often a bottleneck. In addition, due to the increasing importance of deep neural networks, performance models for machine learning applications on HPC systems are of significance. In this thesis we aim to create models for both, providing an extended Roofline model with support for network communication as well as a model specialized for deep neural networks.

For our extended Roofline model, we take the original model's concept of operational intensity and expand it for networked systems with the concept of communication arithmetic intensity. With this, we can model the speed of the interconnect in addition to memory bandwidth for improved prediction accuracy on distributed-memory systems. This model is generalized for all kinds of HPC applications. In the case of the deep neural network model, we use parameterization of collected performance results to predict the execution time. In contrast, this model is highly specific to a particular computer system and application.

For both models we empirically validate them using target applications and systems to determine their effectiveness. The purpose of these tests is to thoroughly determine the prediction quality of the models. For the extended Roofline model, we tested seven algorithms on three computer systems. These are dense matrix-matrix product (SUMMA), 1D fast Fourier transform, a 2D 5-point stencil, Boruvka's minimum spanning tree, dense matrix-vector product, and dot product. The computer systems are Big Red II and Karst at Indiana University, as well as Jetstream from XSEDE. For the neural network model, we tested two networks on two computer systems. The first network is a simple network consisting of only fully-connected layers and activations, and the second network is the widely-known LeNet. The two computer systems we tested are Bridges at the Pittsburgh Supercomputing Center, and Carbonate at Indiana University.

The extended Roofline model improves on the original in nearly all cases that we tested. The best results were achieved for the minimum-spanning-tree algorithm for all three systems, for a percentage improvement of 100%. For the deep neural network model, our best results were achieved for particular layers of the LeNet network on Carbonate and Bridges with an error of 23.43% and 30.24% respectively.

We believe that these two approaches to performance modeling are novel and of interest to those working with both distributed systems and neural networks. To our knowledge, the extended Roofline model is the first extension supporting network communication and the deep neural network model is the first specialized and parameterized model for neural networks. In this sense, we provide both a broad model for HPC in general, and a highly particular model just for machine learning.

2. AN EXTENDED ROOFINE MODEL WITH COMMUNICATION-AWARENESS

2.1 Introduction

Our first goal is producing a performance model that is intuitive and insightful with regard to the balance of floating-point computations, memory accesses and communciation costs. This would allow evaluating new computing platforms and parallel applications. The Roofline model [1] succeeds in being straightforward and easy-to-understand while giving a picture of the balance of floating-point computation and memory operations. The model is both simple and flexible, suggesting that extending it to consider network communication is feasible.

The model is widely used, [2] [3] [4] [5] [6] however, measuring the communication costs of the network is not of its goals. We seek to produce an extension to consider the network as a bottleneck as well as the memory and floating-point bottlenecks. We introduce a new concept, *communication arithmetic intensity* in order to do this. Since this is the communication counterpart of operational intensity, we can now consider all three bottlenecks in a single easy-to-understand visualization. Our model has two primary advantages, simple input parameters and that it is visual.

The first advantage is that the input parameters are simple. The Roofline model has a small number of input parameters that are easy to derive or measure. We carry this over to the new model in order to keep the simplicity. For example, we do not use the latency of the network, the message size, the message receive overhead, or message send overhead. Our communication benchmark is a simple ping-pong test [7]. This benchmark is added to the memory and floating-point benchmarks required by the original Roofline model.

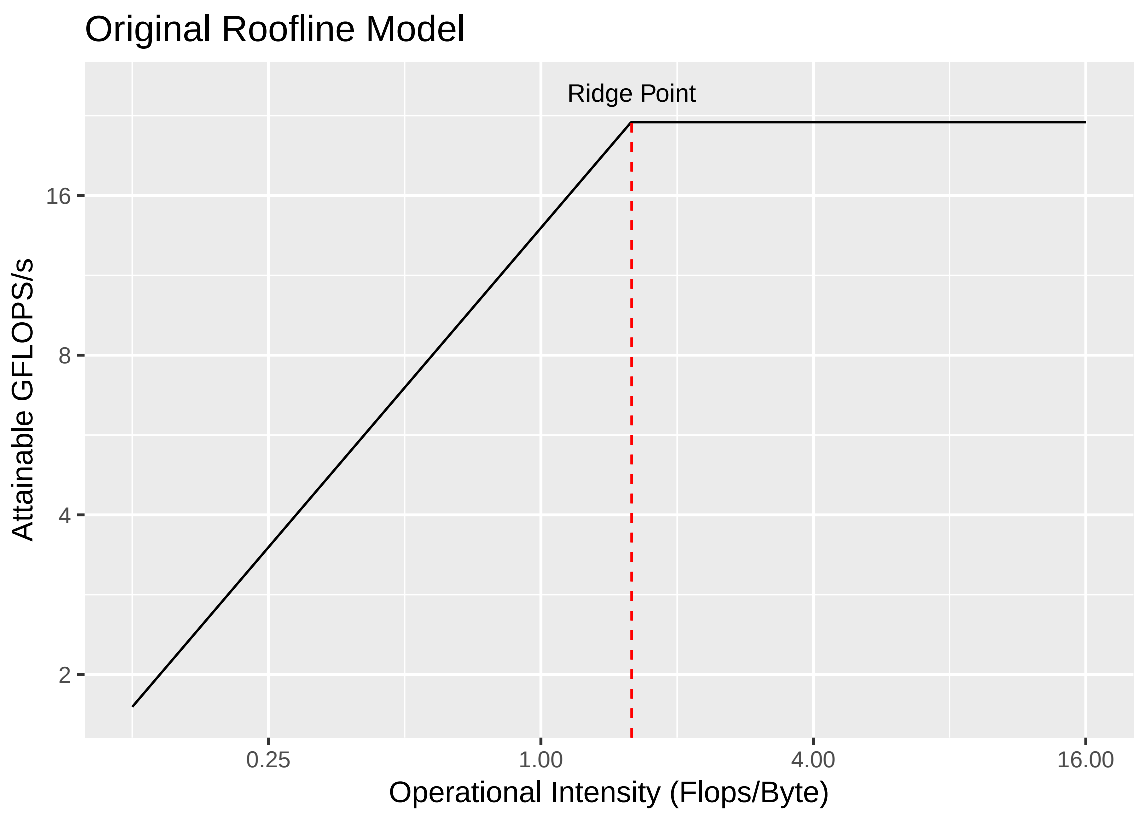

Fig. 2.1. An example of the original Roofline model for the Karst computer system. The ridge point is emphasized with a red dotted line. When the operational intensity increases beyond this location, maximum performance is achieved.

The second advantage is that it is a visual model. This makes it easy to understand. We have both 2D and 3D visualizations of the model. By having both types visualizations two or three bottlenecks can be considered at a time. For example, in the 2D models, we can either visualize the attainable performance vs. the operational intensity, or the attainable performance vs. the communication arithmetic intensity. The 3D model shows the attainable performance, operational intensity and communcation intensity in a single visualization.

Like with the original Roofline model, the *ridge point* is important to understanding the visualization of our new model. An example can be seen in Fig 2.1, where it is the lowest level of operational intensity that can still achieve the highest possible performance. Operational intensities below this point cannot achieve maximum floating-point performance. Since a given algorithm has a particular operational intensity for a particular problem size, we can classify scenarios based on whether they lie to the left or the right of the ridge point, either memory-bound or CPU-bound. This allows us to identify the bottleneck and make a performance prediction. To do this, it is not necessary to run the program on the target hardware. This is true for both the original Roofline model and our extensions.

For the communication visualization in our new model, the ridge point now identifies whether an algorithm is communication-bound or compute-bound. If a communication arithmetic intensity lies to the left of the ridge point, the algorithm is communication-bound. Otherwise, it is compute-bound. By considering this we can classify algorithms in a simple manner.

To demonstrate the model, we evaluated it on seven parallel algorithms to determine the quality of the prediction. We used dense matrix-matrix product (SUMMA), 1D fast Fourier transform, a 2D 5-point stencil, Boruvka's minimum spanning tree, dense matrix-vector product, and dot product. These algorithms cover three of the seven motifs of High Performance Computing [8].

We took these algorithms and tested three different HPC systems. Big Red II represents High Performance Computing, while Karst represents High Throughput Computing and Jetstream represents Cloud Computing. We list the specifications of these systems in Table 2.1.

This chapter makes the following contributions:

- We present an extended Roofline model that considers distributed memory systems with network communication.
- We tested the model with seven algorithms on four computing systems to validate the strength of the prediction. The new model generally achieves a tighter upper bound compared to the original model.

Table 2.1.
The tested systems and their specifications.

	Big Red II	Karst	Jetstream
System Type	HPC	HTC	Cloud
Processor Family	AMD Opteron	Intel Xeon	Intel Xeon
Processor Model	6380	E5-2650	E-2680v3
Cores Per Socket	16	8	12
Sockets Per Node	2	2	2
RAM Per Node	64GB	32GB	128GB
Network	Gemini	10GbE	10GbE
OS	Cray Linux	Red Hat 6	CentOS 7

- We analyzed the efficacy of HPC, high-throughput and cloud systems with regard to these parallel and distributed algorithms.

2.2 Background

The original Roofline model [1] was developed to make a easy-to-understand and straightforward performance model for multi-threaded systems with shared memory. Due to its strengths, it has been used widely. Understanding the relationship between attainable performance and memory bandwidth is difficult, but the Roofline model makes it easier to comprehend.

Equation 2.1 defines the original Roofline model. The peak memory bandwidth is multiplied by the operational intensity, and the minimum of that result is taken with the peak floating-point performance. This gives the attainable floating-point performance.

Operational intensity, as in Equation 2.2, is then designated as the number of floating-point operations divided by the memory bytes transferred. This operational intensity ratio will affect whether an algorithm is floating-point-bound or memory-bound. For example, the BLAS function `dgemm` has a high operational intensity, which indicates that it is floating-point-bound, while `daxpy` has a low operational intensity, which indicates that it is memory-bound.

$$\begin{aligned}&\text{Attainable GFLOPS/s} = Min(\\&\text{Peak Floating Point Performance,}\\&\text{Peak Memory Bandwidth} \times \text{Operational Intensity})\end{aligned} \tag{2.1}$$

$$\text{Operational intensity} = \frac{\text{Floating-point operations}}{\text{Memory bytes transferred}} \tag{2.2}$$

Three examples of original Roofline models are provided in Fig. 2.2-a. The red line represents Big Red II, while blue represents Jetstream, and green represents Karst. On the X-axis we have operational intensity, while on the Y-axis we have the attainable floating-point performance.

2.3 An Extended New Roofline Model

Since the original Roofline model was not developed to consider network communication, we introduce the concept of communication arithmetic intensity. It is defined by Equation 2.3. The peak communication bandwidth is multiplied by the communication arithmetic intensity, and the minimum of that result is taken with the peak floating-point performance. This gives the attainable floating-point performance. Compared to the original model, communication bandwidth replaces memory bandwidth, and communication arithmetic intensity replaces operational intensity.

In the original model, operational intensity uses the memory bytes transferred. Communication arithmetic intensity is defined as the ratio of floating-point operations and the network bytes transferred, as can be seen in Equation 2.4. By doing so, we now have the ratio of network communication to computation the same way the original model has the ratio of memory bytes to computation.

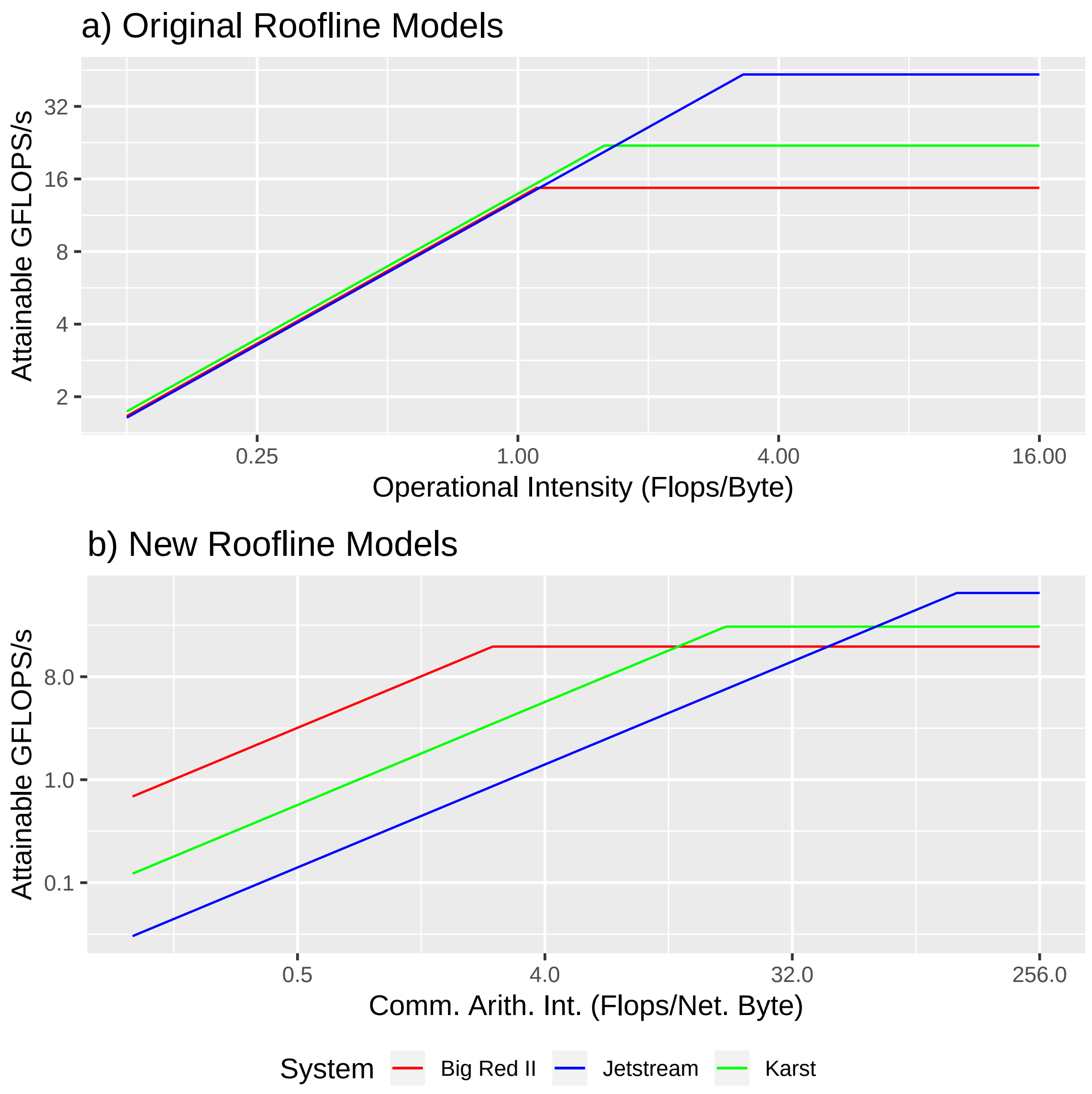

Fig. 2.2. a) This visualization shows the operational intensity graph for the new model. This is identical to the original Roofline model. The three systems are displayed with three distinct lines, with red for Big Red II, blue for Jetstream, and green for Karst. b) The communication arithmetic intensity graph of our new model. We now have communication arithmetic intensity on the X-axis rather then operational intensity.

$$\begin{aligned}&\text{Attainable GFLOPS/s} = Min(\\ &\text{Peak Floating Point Performance,}\\ &\text{Peak Communication Bandwidth} \times \text{Communication Arithmetic Intensity})\end{aligned} \tag{2.3}$$

$$\text{Communication arithmetic intensity} = \frac{\text{Floating-point operations}}{\text{Network bytes transferred}} \tag{2.4}$$

In this model, the ridge point differentiates between communication-bound and floating-point-bound algorithms. Applications with a communication arithmetic intensity to the left of the ridge point need to investigate reducing the number of messages or the size of the messages sent over the network. Otherwise, the algorithm is floating-point-bound and different optimizations need to be investigated. For memory-bound algorithms, we still use the original Roofline model to differentiate. In this sense, the communication Roofline model complements the original Roofline model and adds a new dimension. Using both allows discerning memory-bound, floating-point-bound and communication-bound algorithms.

2.3.1 Limitations of the Model

The original Roofline model simplifies things such as latency and miroarchitectural details to keep the model easy to understand. Similarly, the communication model considers communication to be synchronous and inter-node. We tested applications that mostly use synchronous communication operations such as `MPI_Allgather` rather than asynchronous ones such as `MPI_Isend`. We do not consider latency either, similarly to how the original model does not consider RAM access latency.

2.3.2 Changed Aspects With Respect to the Original Roofline Model

Some versions of the original Roofline model have additional ceilings in the plot to differentiate between FMA or SIMD operations, for example. We have not done this with the communication aspect of the model, and have the communication roofline in a separate plot from the memory roofline. This is done because of the invention of communication arithmetic intensity. In the original Roofline model, FMA or SIMD still use operational intensity and the X-axis is the same regardless. In our model, we use communication arithmetic intensity and the X-axis has changed. Therefore, we cannot superimpose the communication roofline on the memory roofline and keep them both in a single chart.

In addition, a single 2D chart would not be able to differentiate between the three bottlenecks (memory, floating-point, or communication). For this reason, we invented the 3D visualization of our model. The 2D visualization with two charts side-by-side can be considered a projection of the 3D one.

2.3.3 Determining the Model Parameters

As the original Roofline model has operational intensity, peak memory bandwidth, and peak floating-point performance, the communication Roofline model has communication arithmetic intensity, peak network bandwidth, and peak floating-point performance. We derive these from either theory or benchmarks performed on the target system. Peak memory bandwidth, peak floating-point performance and peak network bandwidth are determined with benchmarks, while operational intensity and communication arithmetic intensity are derived with theoretical algorithmic analysis. These parameters are either specific to a system or to an algorithm. The three peak parameters are specific to a system, while operational intensity and communication arithmetic intensity are specific to a particular algorithm. These parameters are summarized in Table 2.2. Derivation refers to whether the parameter is theoretical or taken from benchmark results. Specificity refers to whether the parameter is specific to system hardware or to an application.

In contrast to the original Roofline model, our floating-point and memory bandwidth benchmarks are single-threaded. We model performance from a single MPI process and then extend this to consider multiple threads.

Determining System-Specific Parameters

The three system-specific parameters are peak floating-point performance, peak memory performance and peak network performance. We will explain how to determine them in this section.

Peak Floating-Point Performance: We measure peak floating-point performance by calling the level-3 BLAS `dgemm` function [9]. We use optimized versions from the system vendor and run it single-threaded.

Peak Memory Performance: We measure memory bandwidth with the STREAM benchmark [10]. Of the four algorithms, copy, scale, sum and triad, we select the highest result to attain an upper bound. We run the benchmark in single-threaded mode.

Peak Network Performance: The communication bandwidth was measured with a ping-pong benchmark written by us. After allocating processes to adjacent nodes to minimize latency, we send a message to the second compute node, which responds. We measure the end-to-end time on the first node. By dividing the message size in bytes by half of the end-to-end time we get the point-to-point bandwidth. We used the highest measured performance as the upper bound.

Our benchmark results are displayed in Table 2.3. We use these values for both the original Roofline model and ours.

Table 2.2.
A summary of the five parameters of the model.

Parameter	Derivation	Specificity
Peak Floating Point Performance	Benchmark	System-specific
Peak Memory Bandwidth	Benchmark	System-specific
Peak Communication Bandwidth	Benchmark	System-specific
Operational Intensity	Theoretical	Algorithm-specific
Communication Arithmetic Intensity	Theoretical	Algorithm-specific

Table 2.3.
The benchmark results for the system-specific parameters for our three systems.

System	Memory (GB/s)	Network (GB/s)	GFLOPS/s
Big Red II	13.4	5.7	14.7
Karst	13.9	1.2	22
Jetstream	13.1	0.34	43.4

Determining the Algorithm-Specific Parameters

Operational intensity and communication arithmetic intensity are the algorithm-specific parameters. In this section we describe how to derive them.

Operational Intensity: We take the ratio of floating-point operations to memory bytes transferred. In this scenario, memory bytes refers to bytes transferred to and from RAM. The counting is performed in different ways depending on the algorithm. For some algorithms we count the number of bytes for the inputs and outputs of the algorithm. Other algorithms require more accuracy and we use techniques such as cache-oblivious analysis [11]. We must also count the number of floating-point operations. For this we use asymptotic equations that are widely known.

Communication Arithmetic Intensity : We define communication arithmetic intensity as the number of floating-point operations per byte transferred over the communication link. To determining the number of bytes transferred, we must handle point-to-point and collective communications in different ways.

We simply sum up the size of the messages for point-to-point communications. As an example, we can consider a scenario where a process sends a message of s bytes. If the second process responds with a message of size s, then the total is $2s$ bytes. For asymmetric communications we consider the worst-case to attain an upper bound.

In the case of collective communications, we need to consider the number of stages required to complete the communication. For example, minimum spanning tree-based communications are expected to complete in $\lceil \log P \rceil$ steps [12].

2.3.4 Visualizing the New Model in 3D

Up to this point, we have shown how the communication Roofline model combines with the original Roofline model to produce two figures that allow all bottlenecks to be seen. Next, we will combine the two figures into a single 3D figure. Now, all three bottlenecks will be visible in a single figure.

This 3D model is defined by Equation 2.5. The model has five parameters now. These are communication arithmetic intensity, operational intensity, peak communication bandwidth, peak memory bandwidth, and peak floating-point performance.

$$\begin{aligned}
&\text{Attainable GFLOPS/s} = Min(\\
&\text{Peak Floating Point Performance,} \\
&\text{Peak Memory Bandwidth} \times \text{Operational Intensity,} \\
&\text{Peak Communication Bandwidth} \times \text{Communication Arithmetic Intensity)}
\end{aligned} \tag{2.5}$$

2.4 Related Work

Here we will first discuss previous extensions to the Roofline model, then various methods of network modeling.

2.4.1 Roofline Model Extensions

There have been several previous extensions to the Roofline model, however to our knowledge, none of them consider network communication costs.

Nugteren et al. produced the *Boat Hull* model with the concept of *algorithmic skeletons*. This allows Roofline models to be specialized to particular algorithms that allow analyzing the algorithm before implementing it [13].

Ilic et al. developed a Cache-aware Roofline model [14]. This considers a core-centric approach rather than the chip-centric approach of the original model and considers the cache hierarchy in making performance predictions. We use the definition of operational intensity from this paper in our model in that we consider the total number of bytes of memory traffic rather than the number of off-chip accesses.

A model that considers working set size in embedded systems was developed by Cho et al [15]. While the Cache-aware Roofline model considers the peak performance of the cache, this version also integrates the working set size.

An extension to the Cache-aware Roofline model was produced by Denoyelle et al. to consider NUMA systems. It also has extensions to evaluate the impact of heterogeneous memories. It considers certain types of access patterns such as one-to-all and all-to-all but is limited to a single compute node rather than a distributed system [16].

Latency and out-of-order execution are examples of architectural details added to the model by Cabezas et al. [17]. They also used simulation to schedule instructions and analyze at the cycle level to make performance predictions.

Adding memory latency to the model results in the version produced by Lorenzo et al [18]. Similarly, the extended model suggested by Suetterlein et al. evaluates latency hiding and amortized analysis. They apply it to asynchronous many-task runtimes [19]. While their model includes distributed memory systems and network throughput, their aim is to handle event-driven tasks rather than MPI-oriented programming.

2.4.2 Research Related to Communication Models

One of the earliest models of parallel machines is the PRAM model, which assumes that communication between processors is of zero cost [20]. Unlike the PRAM model we do not differentiate between fast and slow memory, and we consider communication costs.

The BSP model was introduced as a parallel equivalent to the von Neumann model and involves four parameters: the number of processors, the processor speed, the network latency, and the *communication throughput ratio* [21] [22]. The communication throughput ratio is defined as the ratio of the number of words transmitted by the network to the total number of arithmetic operations. The communication throughput ratio bears resemblance to our concept of network operational intensity, but the main difference is that we focus on the computation and communication of a single process rather than the whole system.

The LogP model developed by Culler et al. considers the number of processors, the network bandwidth, the network latency, and the overhead of sending or receiving a message [23]. Unlike the LogP model we do not consider the latency and overhead of sending or receiving messages. Also, unlike the LogP mode we consider the message size.

LogGP extends the LogP model to consider the message size with a linear approximation of the cost of larger messages [24]. Similarly to LogGP, in our model the message size is essential to creating an estimate of the communication intensity of an algorithm.

2.5 Applications

We have selected seven applications to evaluate the model. These are dense matrix-matrix product, 1D fast Fourier transform, 2D 5-point stencil, Boruvka's minimum spanning tree algorithm, dense matrix-vector product, dot product, and Dijkstra's algorithm. All algorithms use MPI for communication and are written in C or C++.

In order to evaluate these applications, we must define the operational intensity and communication arithmetic intensity. The parameters for these are well-known results [25] [26] [27] [28] [29]. These parameters are summarized in Table 2.4.

Generally, we represent the problem size as N, except for minimum spanning tree, where E is the number of edges and V is the number of vertices. The number of MPI processes is defined by P.

We will now introduce the applications:

1. *Dense Matrix-Matrix Product*: We selected this algorithm since it is heavily floating-point-bound. SUMMA is the particular implementation [30]. For reference, this algorithm implements $C \leftarrow \alpha AB + \beta C$ where A, B, and C are double-precision matrices. In our examples the matrices are square and an optimized vendor-supplied `dgemm` is used for the multiplication. In our formula,

the number of elements held in a cache line is specified by B and the cache size in the number of elements is M [25]. For instance, we consider $B = 64/8$ for a 64 byte cache line filled with double-precision elements, and $M = (16 \times 2^{10})/8$, where 16MB is the L1 data cache size on Big Red II.

2. *Vector Dot Product*: We used MPI to implement the parallel vector dot product $x^T y$, where x and y are double precision vectors of size N. This algorithm was selected as representative of a heavily memory-bound algorithm.

3. *1D Fast Fourier Transform*: We perform a FFT operation on a 1D array of complex doubles. The transpose uses additional memory space, meaning that this implementation is out-of-place.

4. *2D 5-Point Stencil*: We selected a stencil algorithm since they benefit heavily from HPC interconnects with low latency. In particular, this small stencil has lower operational intensity in comparison to 7-, 19- or 27-point stencils, meaning that it is more communication-bound.

5. *Boruvka's Minimum Spanning Tree Algorithm*: Boruvka's algorithm determines a minimum spanning tree, which is a classical graph algorithm. It is also heavily communication-bound. This parallel version is based on work by Jahne et al [31].

6. *Dense Matrix-Vector Product*: We have implemented the parallel MPI program to compute $y \leftarrow \alpha Ax + \beta y$ in double precision using the BLAS function `dgemv`. This algorithm was selected as representative of a memory-bound algorithm.

7. *Dijkstra's Algorithm*: This algorithm was selected since it is communication-heavy and a classic graph algorithm.

Table 2.4.
Our derived operational intensity and communication arithmetic intensity formulas used in our models.

Name	Operational Intensity	Communication Arithmetic Intensity
SUMMA	$\frac{(2N^3+2N^2)/P}{(B(1+(N^2/B)+N^3/(B\sqrt{M})))/P}$	$\frac{(2N^3+2N^2)/P}{2\sqrt{P}(8(N/\sqrt{P})^2 \log \sqrt{P})}$
DGEMV	$\frac{(2N^2+2N)/P}{(8N^2+24N)/P}$	$\frac{(2N^2+2N)/P}{8(N/P)(P-1)}$
DDOT	$\frac{2(N/P)-1}{16(N/P)+8}$	$\frac{2(N/P)-1}{8 \log P}$
FFT	$\frac{(5N \log(N))/P}{(48N)/P}$	$\frac{5N \log(N))/P}{32(N/P) \log(P)}$
Stencil	$\frac{4((N-2)/P)(N-2)}{56((N-2)/P)(N-2)}$	$\frac{4((N-2)/P)(N-2)}{32N}$
MST	$\frac{(\lvert E\rvert \log \lvert V\rvert)/P}{(B(Sort(\lvert E\rvert) \log \lvert V\rvert))/P}$	$\frac{(\lvert E\rvert \log \lvert V\rvert)/P}{12\lvert V\rvert(\log \lvert V\rvert/2) \log P+12\lvert V\rvert \log \lvert V\rvert}$
Dijkstra	$\frac{(\lvert E\rvert+\lvert V\rvert \log \lvert V\rvert)/P}{(B(n+(M/B) \log(n/B)))/P}$	$\frac{(\lvert E\rvert+\lvert V\rvert \log \lvert V\rvert)/P}{\lvert V\rvert(16 \log(P))+4(\lvert V\rvert/P) \log(P)}$

Table 2.5.
The tested problem sizes for each algorithm and system.

	Big Red II	Karst	Jetstream
SUMMA	242-61,952		
FFT	256-536,870,912	256-268,435,456	256-67,108,864
Stencil	256-131,072		256-65,536
MST	65,536-67,108,864		
DDOT	256-1,073,741,824		
DGEMV	256-524,288	256-262,144	256-131,072
Dijkstra	256-32,768		256-16,384

2.6 Experimental Results

We will now empirically validate the model by testing on three different systems, which are Big Red II, Karst and Jetstream. These represent High Performance Computing, High Throughput Computing and Cloud Computing, respectively. The specifications of these systems were previously listed in Table 2.1.

2.6.1 Experimental Setup

For each application we will now list the number of iterations, problem sizes, and number of processes. Five trials were ran for SUMMA, MST, and FFT, of which the average time was recorded. In the case of the stencil algorithm, 1000 iterations were timed. Problem sizes increase by powers of two for every problem. Depending on RAM requirements, the sizes differ for each system and algorithm. These are listed in Table 2.5.

Two sets of experiments were performed, one which had multiple processes per node, and one which had one process per node. The single process experiments were performed since MPI used shared memory for local communication, which is significantly faster than network communication. For this reason, both sets of experiments were performed. We allocated processes differently depending on the algorithm and system.

Experiments With A Single Process Per Node

Our simplified SUMMA implementation requires a perfect square process count, so 121 nodes were used on Big Red II and Karst. For other applications, 128 nodes were used. Due to a resource limit of 132 processes, Jetstream was not tested with the single-process-per-node allocation.

Experiments With Multiple Processes Per Node

SUMMA was tested with a total of 1936 processes on Big Red II with 16 processes per node and 121 nodes. With Karst, 576 processes were evaluated with 16 processes per node and 36 nodes.

A difference between the other platform and Jetstream is that the resources are virtualized. We used the largest virtual machine size, m1.xxlarge, which has 44 vCPUs and 120GB of RAM available for usage. The resource limits required us to use three m1.xxlarge instances. For SUMMA, we allocated two nodes with 40 processes and 41 on the third. For the rest, we had two nodes with 43 processes and 42 on the third node.

2.6.2 Comparing With the Original Roofline Model Quantitatively

We wanted to objectively compare the original Roofline model with ours for these results. Therefore, we defined a method for determining their accuracy.

Accuracy Evaluation

The Mean Absolute Percentage Error (MAPE) method is suggested by Equation 2.6 [32]. This gives a process to evaluate the difference between the models. The formula defines n, the number of data points, *actual*, the collected real data, and *predicted*, the model predictions. A smaller error percentage is better and shows that the prediction is closer to the actual data.

$$MAPE = \frac{1}{n} \sum_{t=1}^{n} \left| \frac{actual - predicted}{actual} \right| \tag{2.6}$$

Comparing the New and Old Models

Now that we have calculated MAPE values for each model, we have to compare them. The MAPE values in this case are large and difficult to interpret on their own, so we check the percentage change rather than the raw values. The formula is defined by $100 \times \frac{new - original}{original}$, where *original* is the MAPE value for the original model and *new* is the MAPE value for the new model. The best possible value is 100%. Negative percentages dictate that the new model is worse.

These results are now displayed in Table 2.6. We list each result by the system and algorithm. The largest improvement occurred for MST, with a percentage change of 100% for every platform. DGEMV improved the least with a percentage change of -12.9% on Big Red II.

2.6.3 Interpreting the Figures

We will now evaluate the figures for SUMMA on Big Red II to show how to interpret them.

On the left plot of Fig. 2.3-a we have the communication Roofline model for SUMMA on Big Red II. The X-axis is communication arithmetic intensity, while the Y-axis is the attainable floating-point performance. The red points are the actual performance results. The black line is the Roofline representing a performance prediction of the upper bound attainable at a given communication arithmetic intensity.

Table 2.6.
We display the difference between the original Roofline model and ours in this table.

Algorithm	System	Percentage Change
SUMMA	Big Red II	58.6
SUMMA	Karst	95.1
SUMMA	Jetstream	99.1
1D FFT	Big Red II	90
1D FFT	Karst	98.1
1D FFT	Jetstream	99.4
Stencil	Big Red II	33.3
Stencil	Karst	85.4
Stencil	Jetstream	96
MST	Big Red II	100
MST	Karst	100
MST	Jetstream	100
DGEMV	Big Red II	-12.9
DGEMV	Karst	21.2
DGEMV	Jetstream	89.9
DDOT	Big Red II	75.7
DDOT	Karst	85.1
DDOT	Jetstream	96.6
Dijkstra	Big Red II	87.1
Dijkstra	Karst	98.2
Dijkstra	Jetstream	99.6

For the right side of Fig. 2.3-a, we have the original Roofline model. The X-axis is the operational intensity, while the Y-axis is the attainable floating-point performance. The red points are actual performance results, while the black line is the Roofline predicting the upper bound of attainable performance at a particular operational intensity.

We also have a figure depicting the execution time spent on network communication for each algorithm and platform. If the new model is giving a good prediction of a communication bottleneck, then it should approximately agree with these figures. For example, Fig. 2.4-a shows results for SUMMA. The X-axis is the problem size, while the Y-axis is the percentage of execution time spent on communication. The points represent results for the three platforms, Big Red II, Jetstream, and Karst in red, green and blue.

2.6.4 Results for the Seven Algorithms

Dense Matrix-Matrix Product (SUMMA)

The results for SUMMA are displayed in Fig. 2.3. We can see that the operational intensity is relatively constant at approximately the value 8, as can be seen on the right side of the figure. Lower problem sizes have decreased performance. As the size increases, the performance increases upwards in a close to straight line approaching the Roofline. The original Roofline model does not explain the large change in performance since the operational intensity doesn't change. At any matrix size, the original Roofline model predicts maximum performance since the operational intensity is to the right of the ridge point.

If we evaluate the communication model on the left side of the figure, the communication arithmetic intensity depends on the matrix size. We can see that the result points curve from the left towards the right as the matrix size becomes larger. This occurs since the floating-point operations and network bytes change at different rates as the matrix size increases. Since the algorithm is communication-bound at lower matrix sizes, communication arithmetic intensity explains this phenomenon and the resulting low performance. The original Roofline model does not provide this information. More of the points with low performance are to the left of the ridge point in comparison to the original Roofline model. This results in a better prediction.

If we cross-reference Fig. 2.4-a, we can check that this idea makes sense. In the figure, smaller problem sizes are dominated by the network performance. The ratio of communication time to floating-point time is higher for small matrix sizes than large matrix sizes. Communication time becomes a minority of the total execution time as the matrix size increases.

We improved the prediction by by 58.6%, 95.1% and 99.1% on Big Red II, Karst and Jetstream respectively compared to the original Roofline model. Therefore, our new model improves on the upper bound being predicted.

1D Fast Fourier Transform

We can see the results for the 1D fast Fourier transform in Fig. 2.5. FFT has an operational intensity that changes with the problem size. This stands in contrast to SUMMA, where it is relatively constant. The ridge point is progressed past for this problem on Big Red II and Karst, implying that the application is flops-bound at large problem sizes.

However, we can see that the communication arithmetic intensity gets larger as the input size increases. If we compare the original model to the communication model, the communication arithmetic intensity and operational intensity values are similar for each data point.

The communication model predicts lower performance compared to the original model. The communication arithmetic intensity is lower overall compared to operational intensity, and this applies for each data point. This suggests that the algorithm is less memory-bound than communication-bound. We can cross-reference Fig. 2.4 to see that at small problem sizes, the majority of the execution time is spent on communication, and decreases as the problem size gets bigger. This suggests that our new model is correct.

The percentage change results are 90.0% on Big Red II, while on Karst and Jetstream the change is 98.1% and 99.4%.

2D 5-Point Stencil

We show the Stencil results in Fig. 2.6. The original Roofline model shows that the performance increases as the problem size increases, but the operational intensity is not changing. The original Roofline model does not explain the difference in performance in this situation.

In the communication model, we see that as the problem size increases, the communication arithmetic intensity increases. We can check Fig. 2.4-c to confirm that the percentage of communication time is higher for smaller problem sizes, which causes the communication arithmetic intensity to be higher at larger problem sizes.

The percentage change from the original to the communication model is 33.3%, 85.4%, and 96.0% on Big Red II, Karst and Jetstream respectively.

Boruvka Minimum Spanning Tree (MST)

The results for MST are presented in Fig. 2.7. The operational intensity is larger than the communication arithmetic intensity, which implies that the algorithm is less memory-bound than communication-bound. By checking Fig. 2.4-d, we can see that the amount of execution time spent on communication is relatively unchanged as the problem size increases. The communication model agrees with this since the results have a relatively uniform communication arithmetic intensity.

The communication model produces a good prediction for this algorithm with percentage change values of 100% for all three platforms.

2.6.5 Vector Dot Product

The points in the left-hand plots in Fig. 2.8 display slopes similar to the new Roofline, suggesting that the new model has predictive power. The new Roofline model is able to predict an approximate upper bound proportional to the collected data.

The differences between the left-hand and right-hand plots in Fig. 2.8 indicate that there is a great error reduction for all three computing systems since the plotted points are closer to the new Roofline than the original Roofline. For example, the error percentage on Big Red II is reduced by 75.7%.

2.6.6 Matrix-Vector Product

The results for DGEMV are displayed in Fig. 2.9. By examining Fig. 2.4-e we can see that the communication time is greater for smaller sizes than larger sizes.

2.6.7 Dijkstra's Algorithm

The results for Dijkstra's algorithm are displayed in Fig. 2.10. By examining Fig. 2.4-g we can see that communication time dominates the execution time on all platforms and sizes.

2.6.8 Multiple Process Per Node Results

Our experiments in the previous section user one process per node on Karst and Big Red II. However, real-world applications use multiple processes per node, so me must validate this scenario as well. Jetstream is not included in this section since it already used multiple processes per node in the previous section.

We display the results for SUMMA in Fig. 2.11. The original Roofline prediction is similar to the single-process-per-node result, where maximum performance is predicted for all problem sizes. The communication model gives a better prediction since some of the matrix sizes are predicted to be communication-bound. The model works since collective MPI operations are blocking. The communication arithmetic intensity is higher than the operational intensity for most of the data points. The process allocation results in more performance since less data is being transferred over the network.

2.7 Results With the 3D Model

Now we will examine the 3D visualization of our model, first with a comparison of the three platforms used in this paper. Then we will explore the results for SUMMA with the 3D model.

2.7.1 3D Models for the Three Systems

The 3D Roofline models for the three systems are displayed in Fig. 2.12. The Z-axis represents the attainable floating-point performance, while the Y-axis represents communication arithmetic intensity, and the X-axis represents operational intensity. These are abbreviated as `At. GF/s`, `C.A.I.` and `Oper. Int.` respectively. The range of the axes extends to the minimum operational intensity and communication arithmetic intensity required to reach maximum performance on Jetstream. That way, the systems are easy to compare.

Rather than Rooflines, we now have planes. There are three planes representing the maximum attainable performance under the influence of three bottlenecks. We will describe these by their position in the image, left, right and top. The top plane represents combinations of operational intensity and communication arithmetic intensity that result in a floating-point-bound algorithm. For this reason, the plane rises higher than the other two. The right plane represents algorithms that are bound by network bandwidth. The left plane represents algorithms bound by memory bandwidth. As operational intensity increases, data points will ascend the memory-bound plane and attain maximum performance as they transition to the floating-point-bound plane.

These factors combined produce a single visualization that considers all three bottlenecks for a full picture of a particular system's performance. For example, an algorithm with low operational intensity and high communication arithmetic intensity is going to be memory-bound. Therefore, ways to reduce memory accesses must be found to improve the performance of the application.

By comparing the right planes of the systems we can see that since each system has a different level of network performance, the slopes of the planes are steeper or gentler. For example, Jetstream requires the highest communication arithmetic intensity to achieve maximum floating-point performance, therefore the slope of the right plane is the gentlest. On the other hand, Big Red II has the fastest network performance and therefore has the steepest right plane. Karst lies in the middle with a network performance that is inbetween the other two systems. We can check Table 2.3 to verify that these characteristics match the stated performance of the hardware.

With the case of memory bandwidth, the systems are similar. This is reflected in the left planes, that all have similar slopes.

The last bottleneck that must be considered is the floating-point bottleneck. In this case, the top planes are all significantly different for each system. They either lie higher or lower depending whether the maximum performance is better or worse. Big Red II has the lowest floating-point performance and therefore the lowest plane. Karst has a middle level of performance, and Jetstream has the highest.

2.7.2 SUMMA Results in 3D

We will now examine the results for SUMMA in 3D in Fig. 2.13. We once again have the Roofline planes for each system in subfigures a, b, and c. The models generated Fig. 2.12 are now superimposed with performance result points. The models look somewhat different from the previous figure since the range of the axes has changed. They range from 0 to the maximum operational intensity or communication arithmetic intensity value for a given application in this case. We have also subdivided the colorization of the figures differently. The subfigures in Fig. 2.13 are divided into 64 segments, while the subfigures in Fig. 2.12 are divided into 128 segments. The purpose is to make the result points easier to see, which are the same as in the 2D results. They approximately approach the bottom of the surface, showing that it makes an upper bound like in the 2D results.

2.8 Conclusion

In summary, we have extended the Roofline model to make performance predictions for parallel applications on distributed memory systems. To achieve this, we added a new dimension of communication amounts to the model while retaining the memory performance predictions of the original model. The model was validated by performing an empirical study with different algorithms and computing systems that represent three different paradigms of computing. These are high performance, high throughput, and Cloud computing. We retain the simplicity of the original model in the new model and provide two ways of visualizing the results in both 2D and 3D. This provides an intuitive way of understanding the performance of distributed-memory systems and their applications.

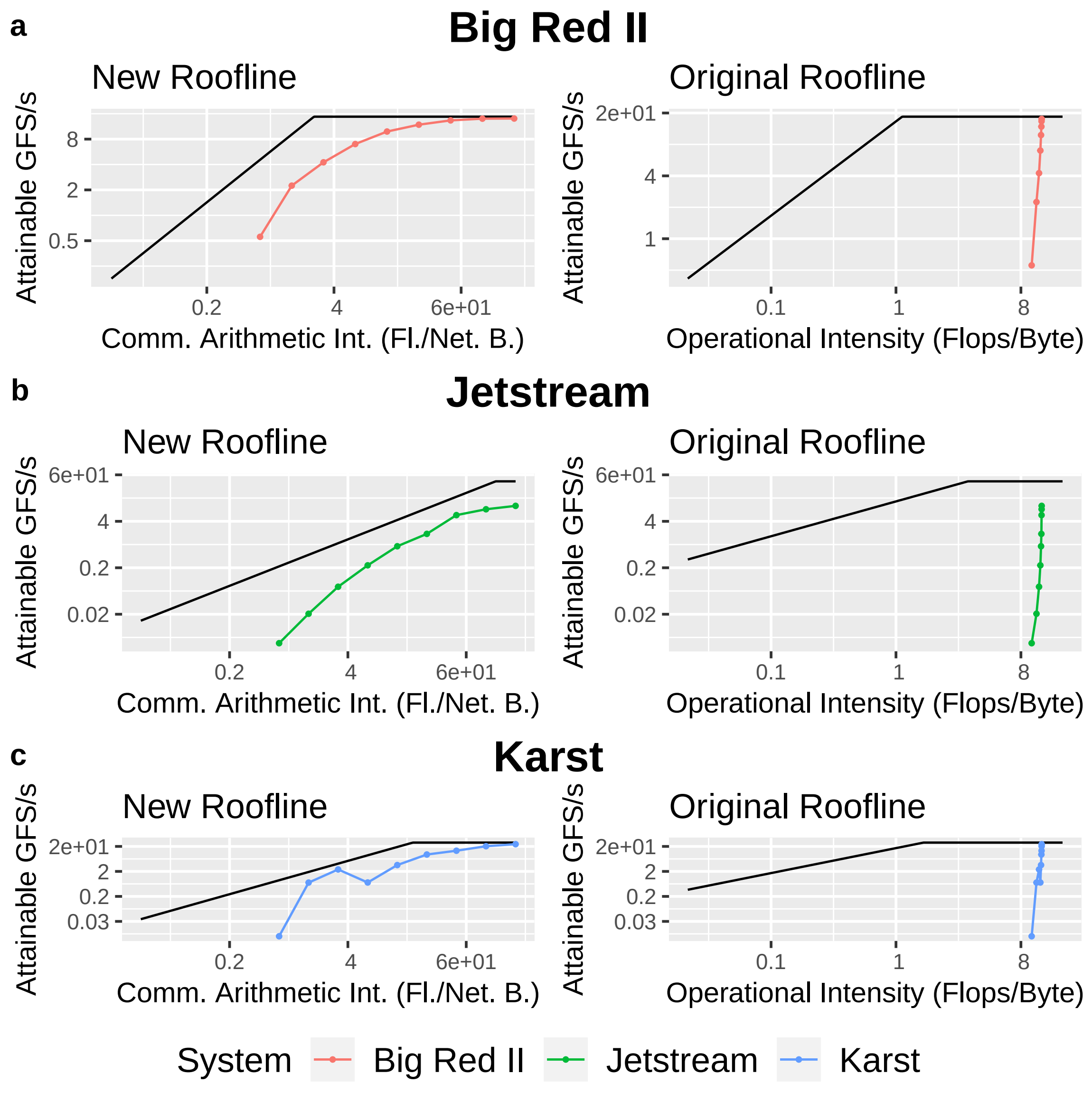

Fig. 2.3. Here we show the 2D visualization of the new model. Note that the operational intensity Roofline model is the same as the original Roofline model. We display Big Red II in a, Karst in b, and Jetstream in c. The performance upper bound is signified by the black line, while the colored points represent actual performance measurements for various problem sizes. The points are connected by lines for clarity. The performance points are the same for the left and right representations and give different views on the same data according to our new model. Beware that the X- and Y- scales are not the same among plots.

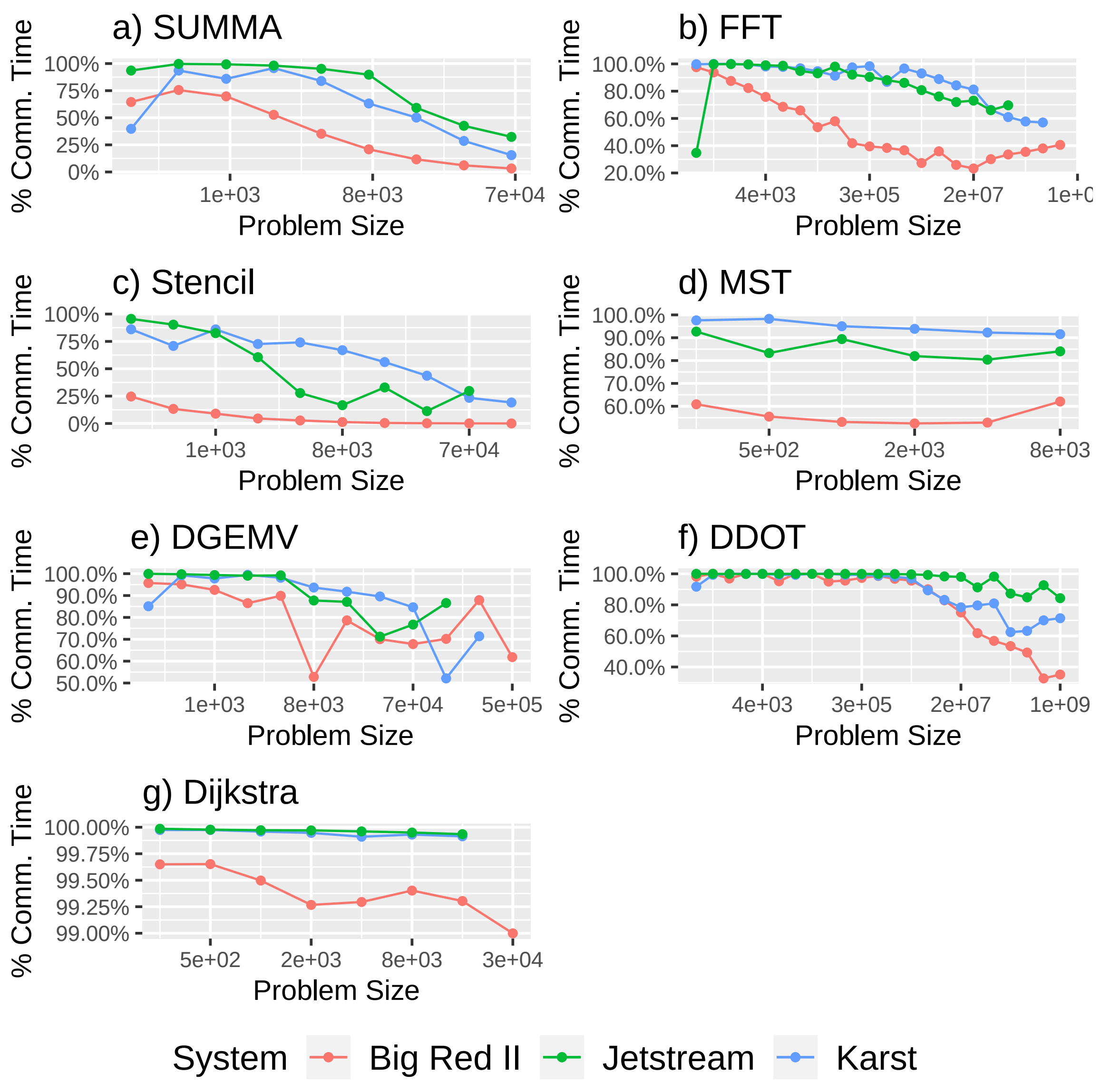

Fig. 2.4. Here we display the ratio of communication for the computer systems and algorithms. Red points represent Big Red II, blue points represent Karst, and green points represent Jetstream. Chart a) represents SUMMA, b) represents FFT, c) represents Stencil, and d) represents MST. On the X-axis is the problem size, while the Y-axis represents the percentage of time spent on communication. We used one process per node for Big Red II and Karst, giving a total of 121 SUMMA processes and 128 for the other algorithms. On Jetstream, we used 3 nodes for SUMMA. The processes were divided such that two nodes had 40 processes and the third had 41. This resulted in a total of 121 processes. The other three algorithms used an allocation of 43 processes on two nodes and 42 on the third. This resulted in a total of 128 processes.

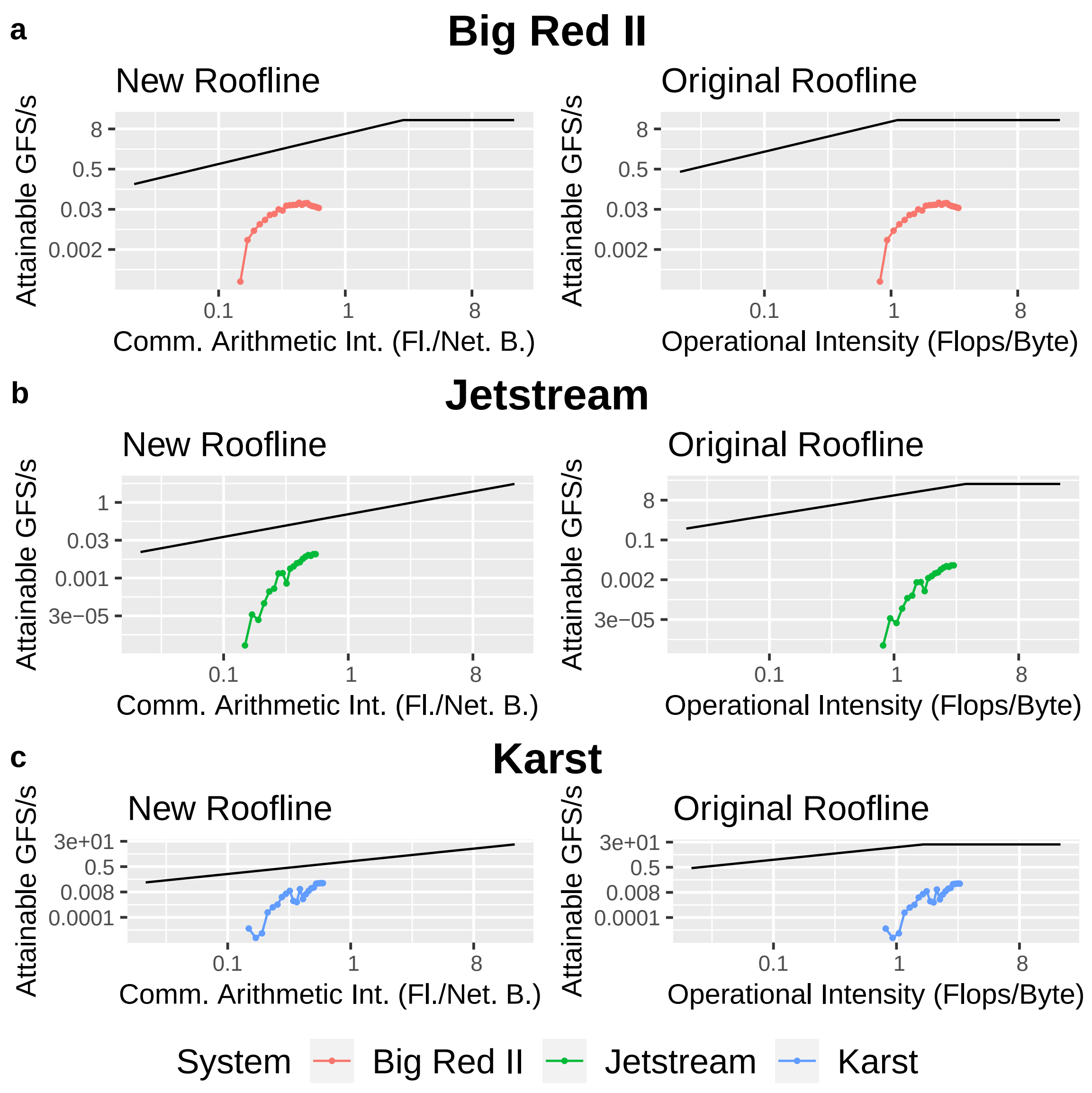

Fig. 2.5. The operational intensity and communication diagrams for FFT.

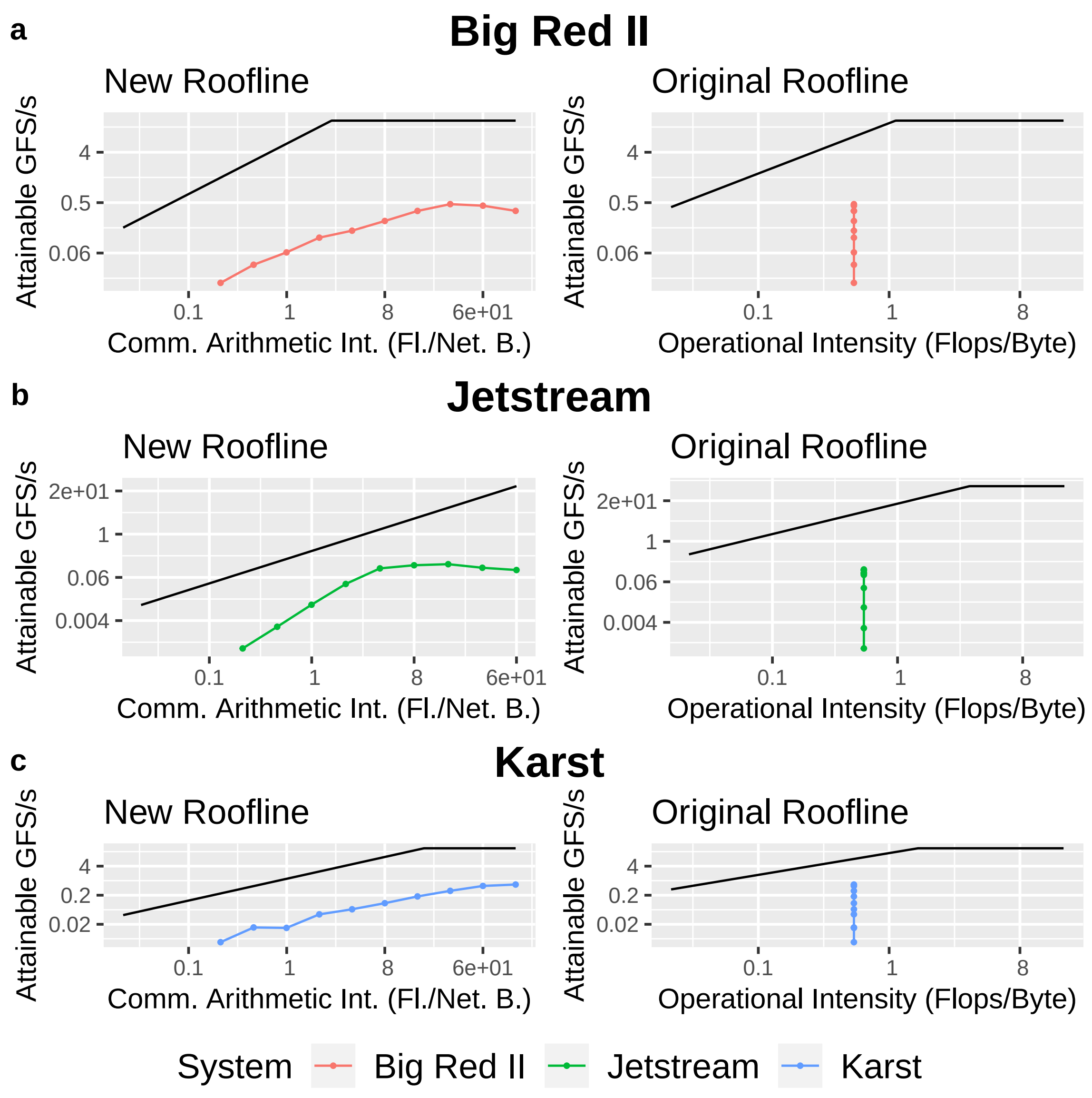

Fig. 2.6. The operational intensity and communication diagrams for Stencil.

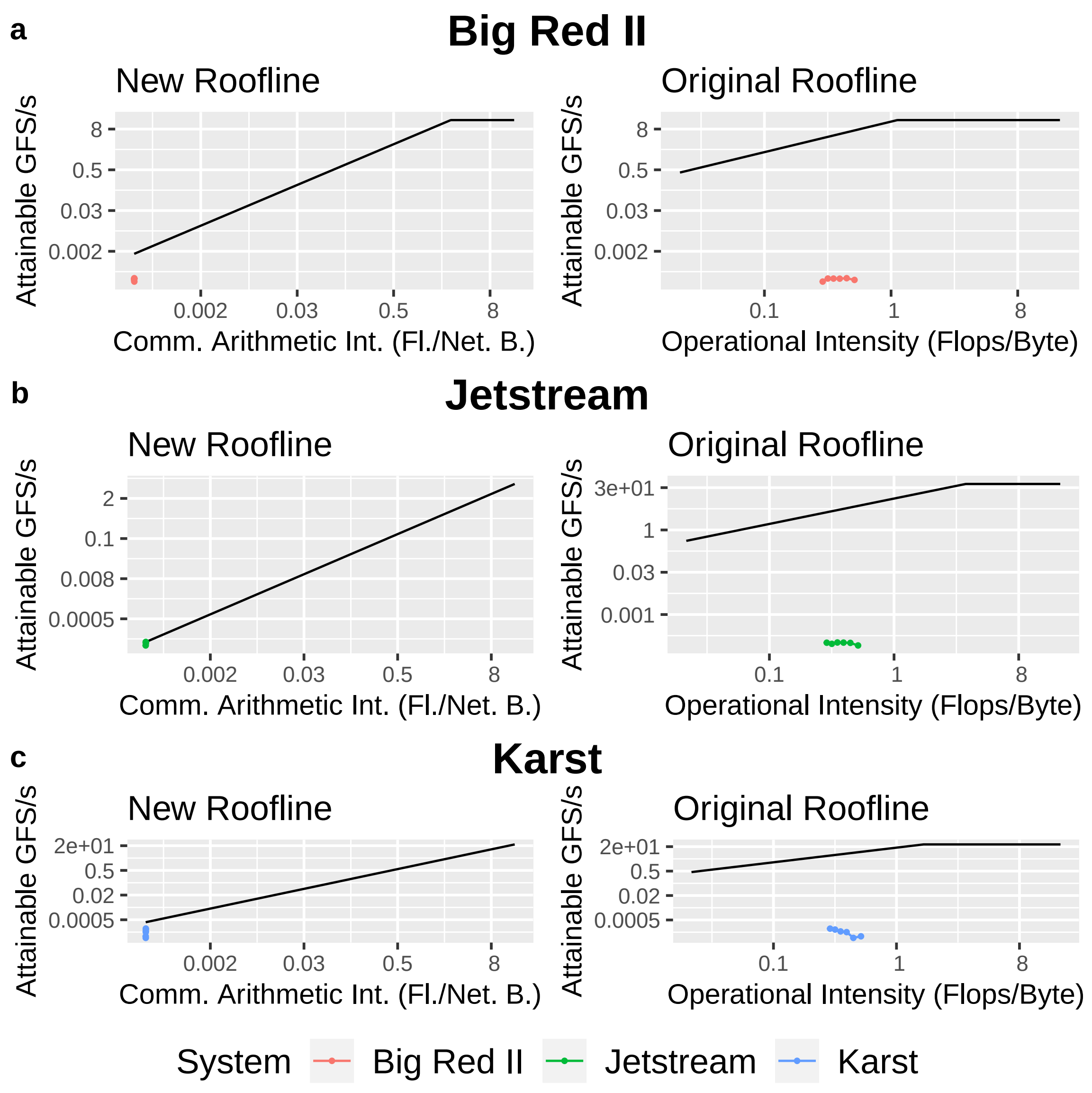

Fig. 2.7. The operational intensity and communication diagrams for MST.

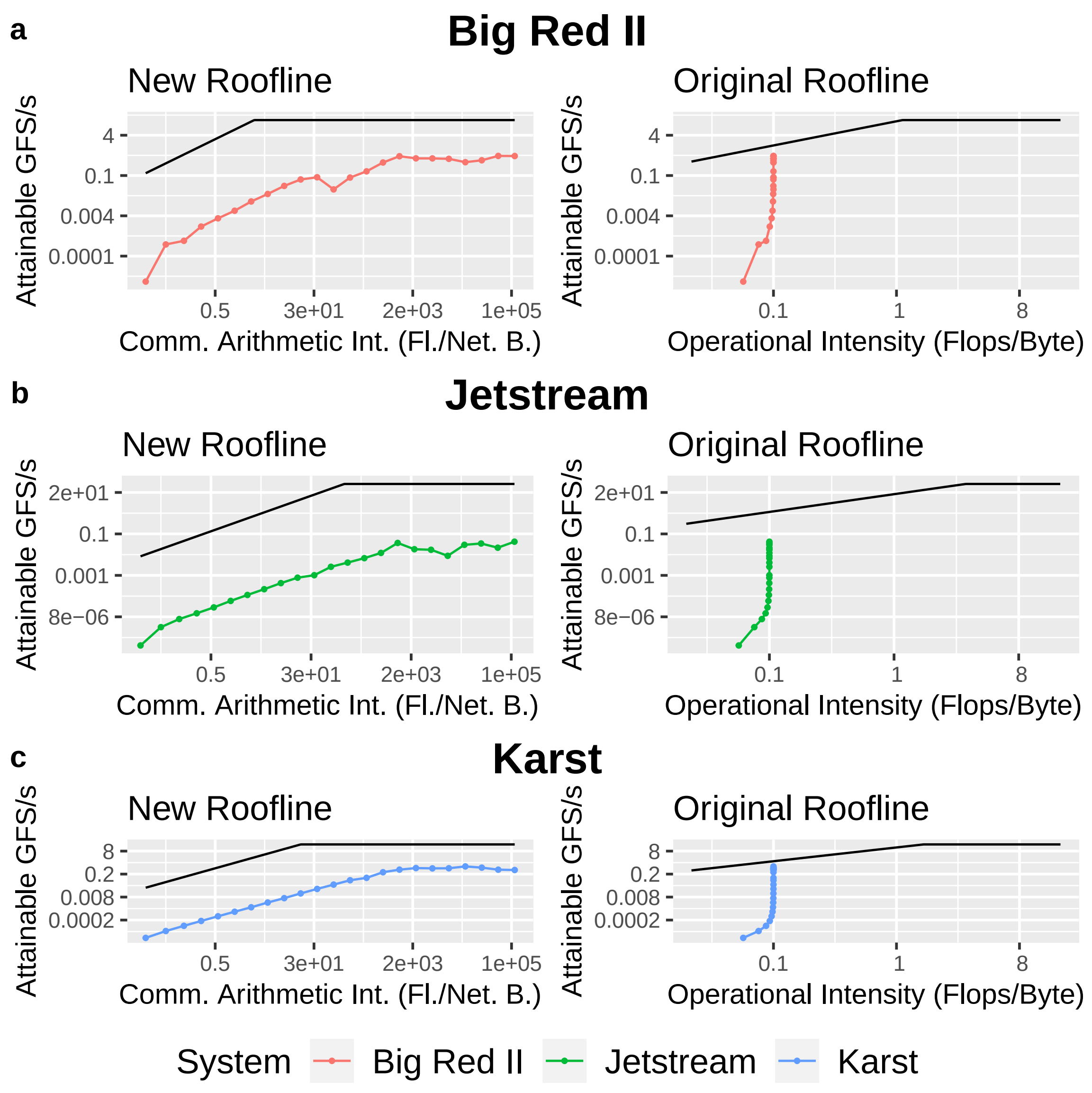

Fig. 2.8. The operational intensity and communication diagrams for DDOT.

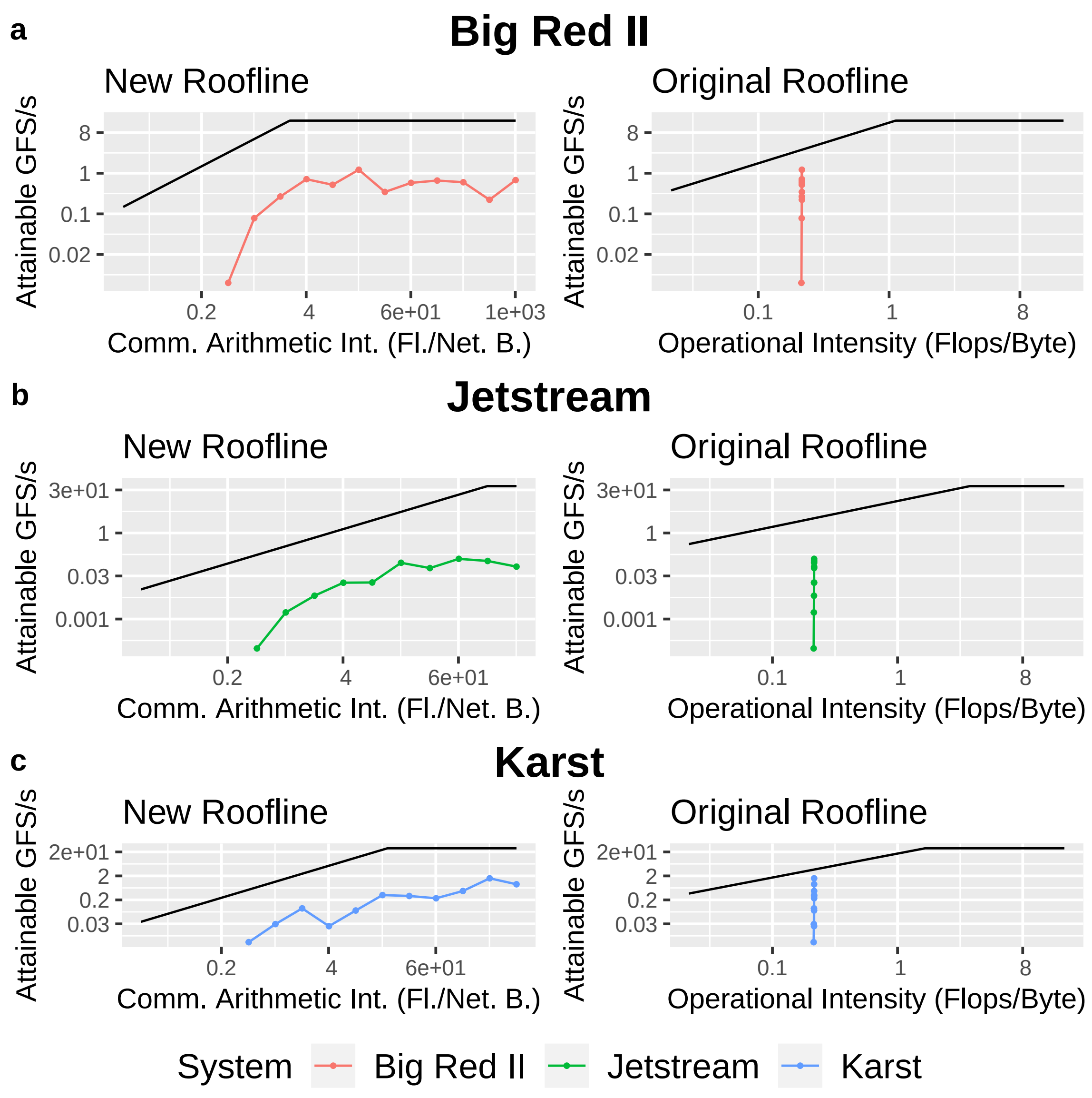

Fig. 2.9. The operational intensity and communication diagrams for DGEMV.

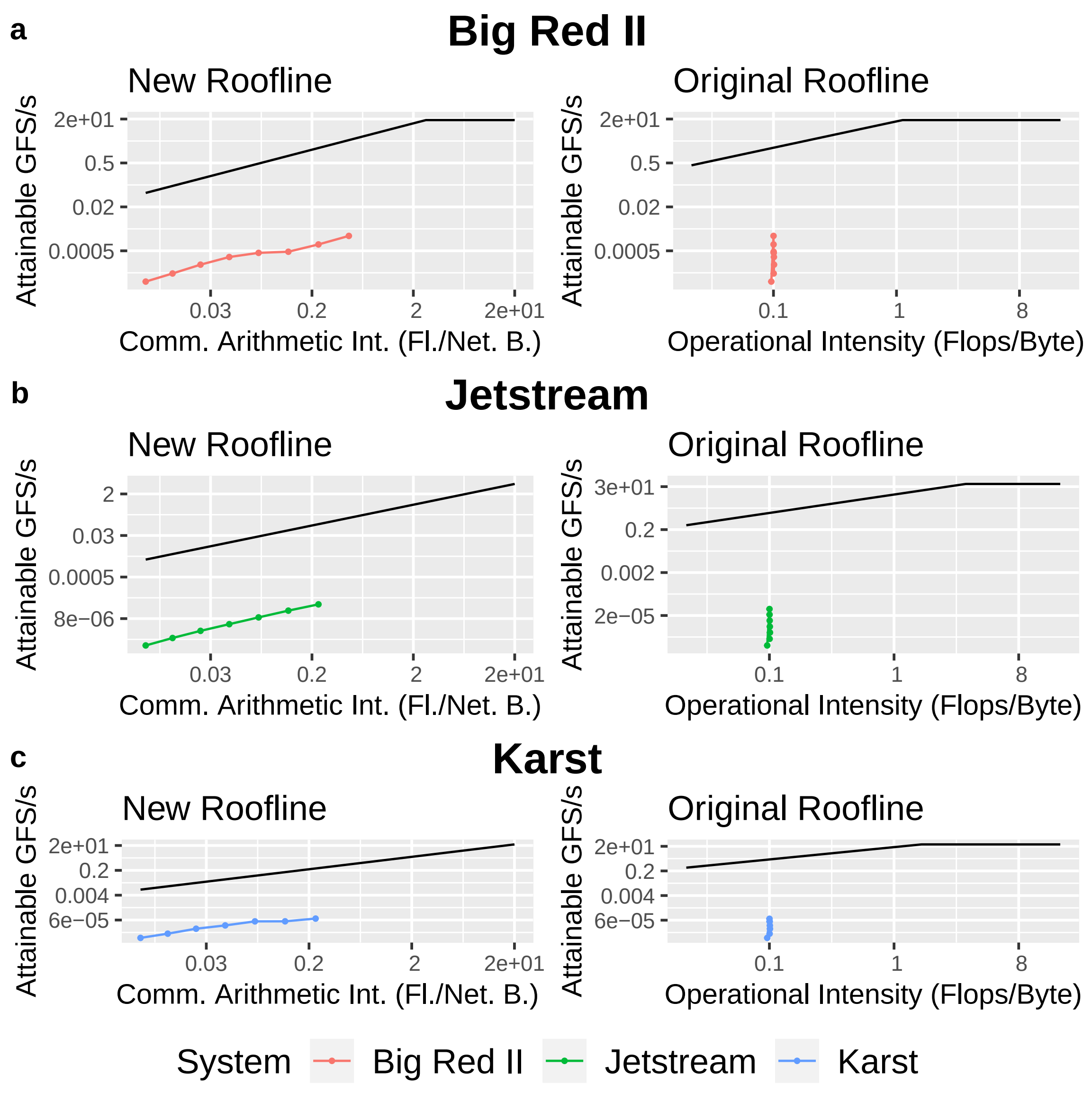

Fig. 2.10. The operational intensity and communication diagrams for Dijkstra.

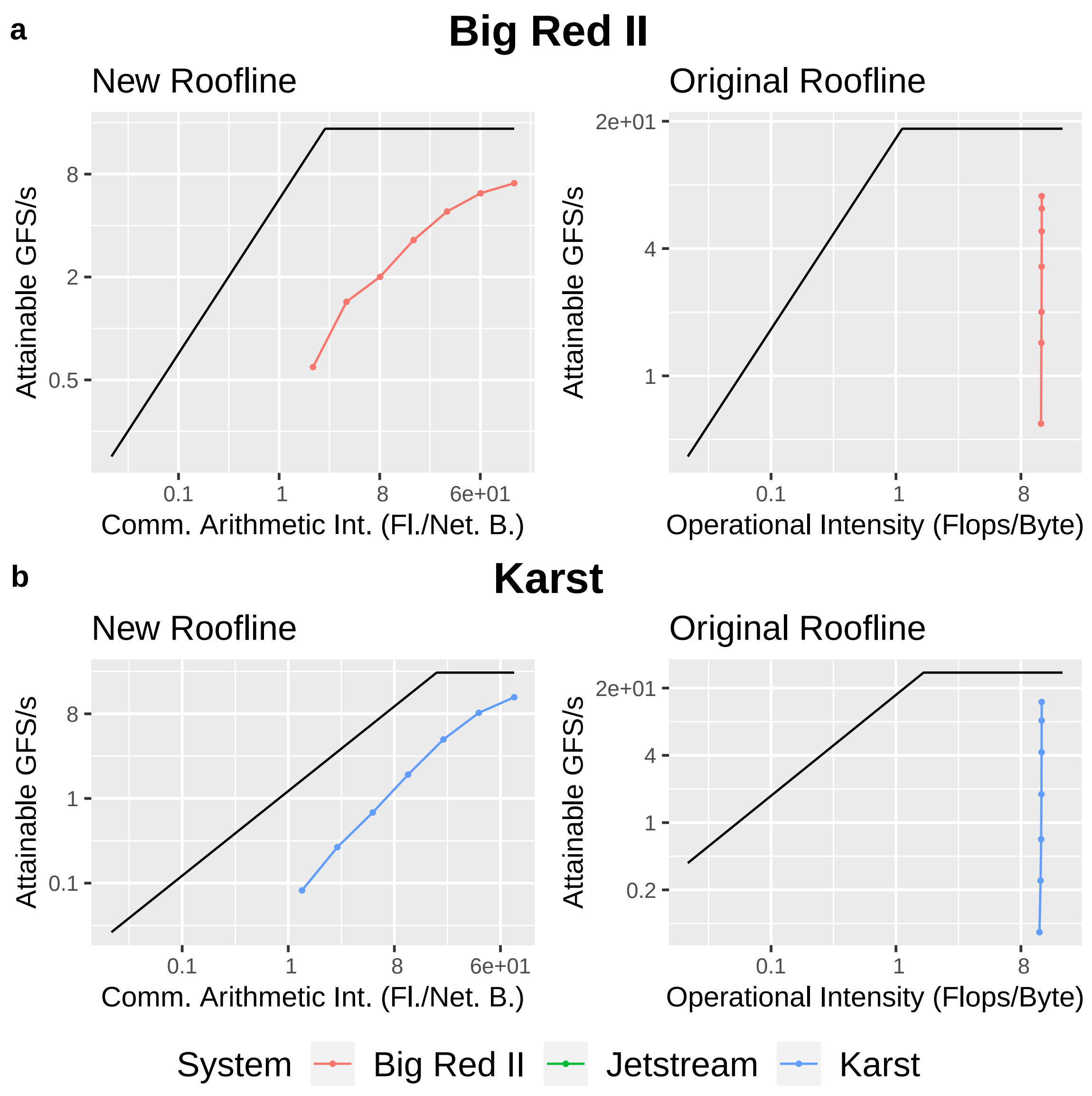

Fig. 2.11. For SUMMA, we display the multi-process results here.

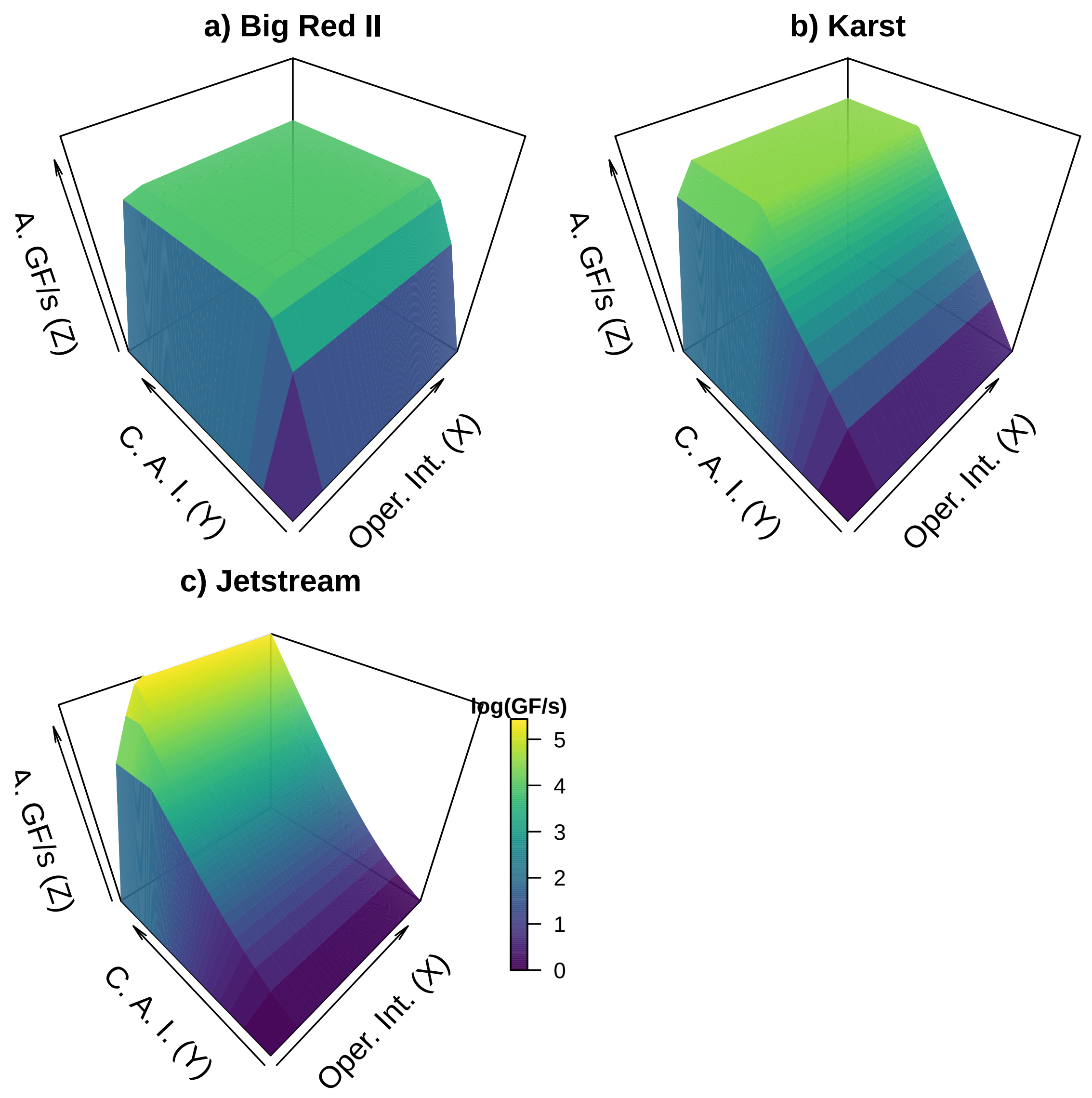

Fig. 2.12. We can compare the three systems using the 3D model. Plots a, b, and c represent Big Red II, Karst and Jetstream respectively. GFLOPS/s is represented by the Z-axis, while communication arithmetic intensity (C.A.I) is on the Y-axis. The X-axis represents operational intensity (Oper. Int.). Lighter colors represent higher performance, while darker colors represent lower performance. It should be noted that this plot is logarithmic.

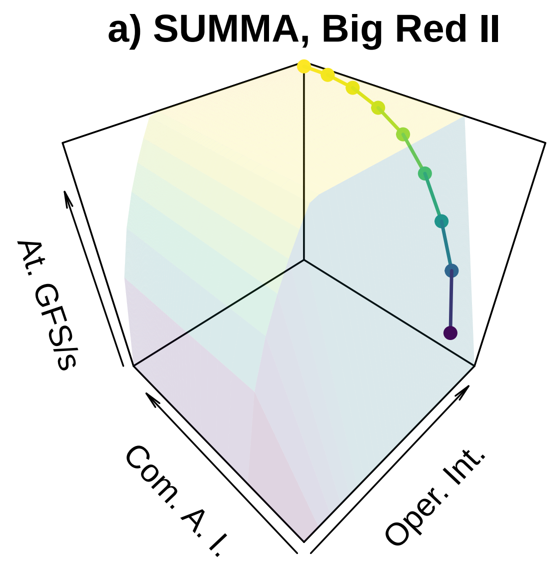

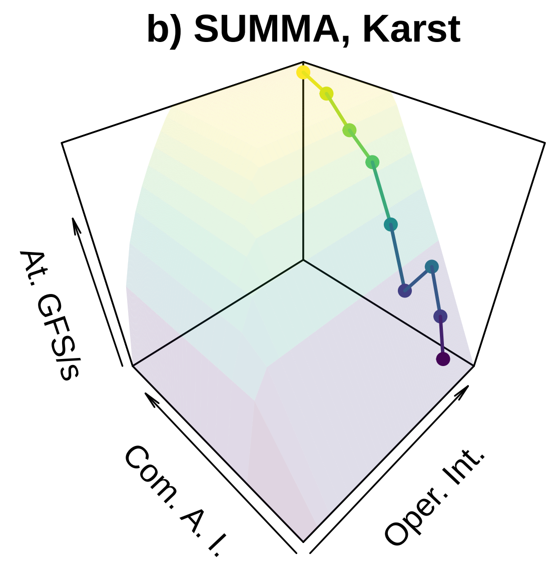

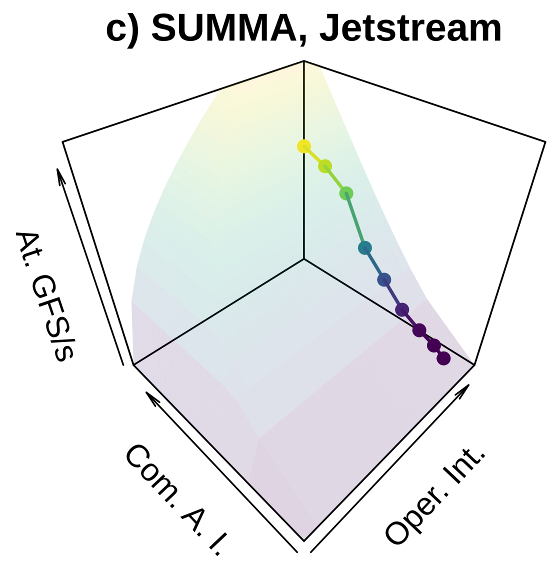

Fig. 2.13. Results for SUMMA plotted using the 3D visualization. Plots a, b, and c represent Big Red II, Karst and Jetstream respectively. Performance results are plotted using points.

3. A PARAMETERIZED PERFORMANCE MODEL FOR DEEP NEURAL NETWORKS

3.1 Introduction

Deep learning has developed as a powerful tool for modeling tasks, however the computation time required is high. For this reason, it is increasingly a core part of High Performance Computing and methods for understanding and accelerating the performance would be of interest. In pursuit of models with higher prediction accuracy we present a parameterized Roofline model specialized for deep neural networks. By parameterized, we mean that our model uses performance results for given input sizes to make predictions. This is inspired by the the parameterized LogP model by Kielmann et al [7]. We present our new model and perform an empirical analysis of it on target machines using a C++ implementation of neural networks to evaluate its efficacy.

3.2 Background

In deep neural networks, a single neuron can have inputs and outputs with an activation function. These neurons are grouped in layers, and these layers are chained from one to the next to create a deep number of layers. In this sense, hierarchical features can be learned by the network from the input data, enabling complex applications. Each layer has a forward pass, back-propagation and a weight update phase. In this paper, we are primarily concerned with a few fundamental layers and processes that take the most computation time, of which the most important is the fully-connected layer.

3.2.1 Fully-Connected Layer

A fully-connected layer is defined by the function $y = f(xW + b)$, where x is a matrix of inputs, W is a matrix of weights, b represents the bias vector, and f, the activation function. The two activation functions used in this paper are ReLU and sigmoid. ReLU is defined as $R(z) = max(0, z)$, while sigmoid is defined as $S(x) = \frac{1}{1+e^{-x}}$. For our purposes in this paper, we care about the cost of the multiplication of the weights and inputs, adding the bias vector, and applying the activation function.

3.3 Our Model

To achieve higher prediction performance, we extend the original Roofline model by parameterizing the peak floating-point-performance parameter. For each performance prediction, we derive the peak by taking a dense multiplication performance result of a particular size and using that as the Rpeak parameter. Our model is defined by Equation 3.1.

$$P = \min\{f(k, m, n), OI \times Mpeak\} \tag{3.1}$$

P represents the peak achieved performance predicted by the model. We take the minimum of the parameterized performance result for given matrix of size k, m and n and the operational intensity times the maximum memory bandwidth. The function f represents this particular performance result. OI represents operational intensity, the number of flops per byte transferred to and from memory and is defined in Equation 3.2.

$$OI = \frac{F}{M} \tag{3.2}$$

Table 3.1.
The layer weight sizes and output sizes for the simple network.

Layer	Weights	Outputs
Fc1	50x784	$\beta x50$
Fc2	10x50	$\beta x10$

3.3.1 Network Modeling

We studied one network, a simple one consisting of a fully-connected layer with ReLU activation, followed by a fully-connected layer and sigmoid activation. The first layer of the simple network has a fully-connected layer with bias and a ReLU activation. It has 784 inputs and 50 outputs. The input to the network is of size $\beta x1x28x28$ where β is the batch size. This input must be reshaped to $\beta x784$ to be input into the 1st fully-connected layer. Therefore the first operation is multiplying the $\beta x784$ by the transposed weights of size 784x50 to get a $\beta x50$ result. Then, we must add the bias. For the 1st fully-connected layer this is a vector of size 50. Since this vector is added to every row it is $\beta x50$ add operations. Finally, we must apply the ReLU activation. Since this must be performed on every element of the output matrix we consider it to be another $\beta x50$ add operations.

For the second layer there are no real differences with the first except the sizes. Our input into the second fully-connected layer is $\beta x50$ and the weights are 10x50. This gives the first operation as a $\beta x50$ by 50x10 multiplication to give a $\beta x10$ output. Bias is applied, adding another $\beta x10$ operations, then sigmoid is applied, giving another $\beta x10$ operations.

3.4 Related Work

Calotoiu et al. developed a multi-parameter performance model using performance model normal form to handle the effects of the interaction of the problem size and number of processors [33]. Their model uses linear regression unlike ours.

The concept of algorithmic profiling was introduced by Zaparanuks et al. by generating cost functions to consider the asymptotic cost of algorithms [34]. Instead of using performance results of similar functions like our work, they perform an algorithmic analysis.

Yan et al. developed a performance model suitable for distributed deep learning to estimate the epoch time for a given network and system configuration [35]. However, their model starts from timing a single multiply-add operation and extrapolates from that, rather than the full multiplications and additions for a given problem size.

A performance modeling method for determining the iteration time of CNNs for multi-GPU setups was developed by Pei et al [36]. Similar to their method, we determine the cost of each layer per-iteration. However their method primarily concerns GPUs and TensorFlow while we focus on CPUs and our C++ implementation of neural networks.

3.5 Test Systems

We evaluated the performance of the model on two systems, Carbonate at Indiana University and Bridges at the Pittsburgh Supercomputing Center [37]. The specifications of the systems are displayed in Table 3.2.

3.6 Parameters

This model requires the peak memory performance measurement as in the original Roofline model. For this we used the STREAM benchmark. We measured the peak bandwidth of Carbonate at 12,937.6 MB/s, while Bridges had 11,442.7 MB/s.

Table 3.2.
The tested systems and their specifications.

	Carbonate	Bridges
Processor Family	Intel Xeon	Intel Xeon
Processor Model	E5-2680 v3	E5-2695 v3
Cores Per Socket	12	14
Sockets Per Node	2	2
RAM Per Node	256GB	128GB
Network	10GbE	10GbE
OS	Red Hat	Red Hat

The parameterized performance results were collected with our C++ library at various matrix sizes. On Carbonate we used OpenBLAS for the matrix multiplication routines, while on Bridges we used MKL. The microbenchmark results are listed in Tables 3.3 and 3.4 for Carbonate and Bridges respectively. M, N, and K represent the dimensions of the matrix multiplication measured. Time is the measured time in seconds.

3.7 Experimental Setup

With the parameter data collected, to empirically validate the model we tested in several configurations. We varied the batch size between 32, 64 and 128 to see if the model is able to handle various batch sizes. Therefore between the two systems and three batch sizes we have six results to present in total.

3.8 Results

We tested the model on two computing systems, Carbonate and Bridges. We will present those results in this section. The meanings of the abbreviations in the result

Table 3.3.
Microbenchmark results for Carbonate.

M	N	K	Time
32	784	50	0.000143
32	784	10	0.000074
32	50	50	0.000015
32	50	10	0.000005
64	784	50	0.000157
64	784	10	0.000050
64	50	50	0.000030
64	50	10	0.000010
128	784	50	0.000207
128	784	10	0.000064
128	50	50	0.000064
128	50	10	0.000027

tables are summarized in Table 3.5. The results are summarized using MAPE in 3.8. The results are organized by the test system, the batch size, and the resulting mean absolute percentage error value. Lower MAPE values are better.

3.8.1 Carbonate

The results for the simple network on Carbonate are displayed in Figure 3.1. The X-axis shows the layers or operations listed by type. These operations are the first fully connected layer, the second fully connected layer, the ReLU activation, and the sigmoid activation. The Y-axis shows the time in seconds. The actual results are in red, while the parameterized predictions are in blue. Each panel shows a different batch size, which are 32, 64 and 128.

Table 3.4.
Microbenchmark results for Bridges.

M	N	K	Time
32	784	50	0.000102
32	784	10	0.000028
32	50	50	0.000011
32	50	10	0.000003
64	784	50	0.000169
64	784	10	0.000046
64	50	50	0.000019
64	50	10	0.000005
128	784	50	0.000326
128	784	10	0.000102
128	50	50	0.000041
128	50	10	0.000010

These results are shown again in Table 3.6 with their absolute percentage error values. The results are sorted by the batch size. The actual time for a layer, predicted time and absolute percentage error are displayed. The most accurate prediction was made for the first fully-connected layer at batch size 128 for an absolute percentage error of 0.49%. The overall best prediction on Carbonate was for a batch size of 128 with a MAPE value of 44.36%.

3.8.2 Bridges

The results for the simple network on Bridges are displayed in Figure 3.2. The corresponding Table 3.7 displays the results with their error values. At an absolute percentage error of 6.59%, the first fully-connected layer at batch size 128 was the

Table 3.5.
The meaning of each column in the result graphs.

Abbreviation	Meaning
fc1	Fully-connected 1
fc2	Fully-connected 2
relu	ReLU
sigmoid	Sigmoid

most accurately predicted. Of the three batch size configurations, batch size 64 was the most accurately predicted overall with a MAPE value of 52.88%.

3.9 How the Model Improves Prediction Quality

We will look at a particular example from our results to display how the model improves prediction quality. For the 1st fully-connected layer with batch size 128 on Carbonate, we achieve a 0.49% error. In the first step, we fetch the appropriate performance result for a 128x784 by 784x50 multiplication. This is 0.000207 in our particular case. We convert this to GFLOPS/s by considering the number of floating point operations, which is 5,017,600, giving 242.3 GFLOPS/s. This is our new RPeak. We consider there to be $128 \times 784 + 784 \times 50 + 128 \times 50$ memory operations, which gives an operational intensity of 34.3. We multiply the operational intensity by the memory peak, which is 12,937.6, which after a conversion, gives 444.7 GFLOPS/s. This is larger than the previously calculated 242.3 GFLOPS/s so we select it, giving our accurate prediction.

3.10 Conclusion

We developed an extended parameterized Roofline model for deep learning and validated it with various configurations and systems. Since our performance model uses parameterized performance results, it achieves higher accuracy in performance prediction for deep neural network applications. Our best prediction for a single layer was 0.49% error, while the best result for a particular network configuration was a 44.36% MAPE value.

Table 3.6.
Results for the simple network on Carbonate.

Type	Batch Size	Actual	Predicted	Absolute Percentage Error
fc1	32	0.000103	0.000143	38.83
relu	32	0.000033	0.000000	98.50
fc2	32	0.000008	0.000005	37.50
sigmoid	32	0.000011	0.000003	73.02
fc1	64	0.000249	0.000157	36.95
relu	64	0.000066	0.000001	98.50
fc2	64	0.000013	0.000010	23.08
sigmoid	64	0.000022	0.000006	73.02
fc1	128	0.000206	0.000207	0.49
relu	128	0.000144	0.000002	98.63
fc2	128	0.000028	0.000027	3.57
sigmoid	128	0.000047	0.000012	74.74

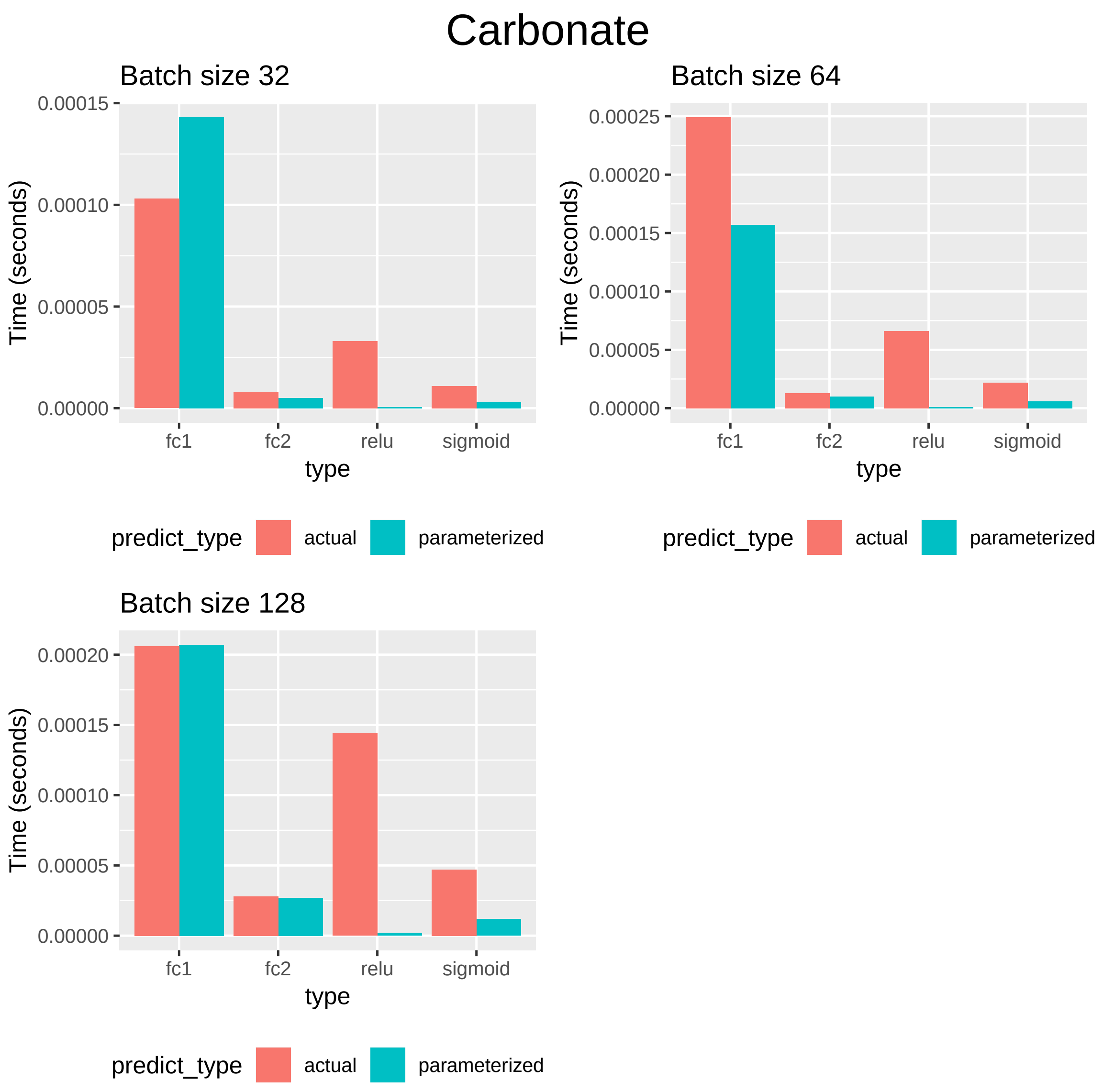

Fig. 3.1. Results for the simple network on Carbonate. The actual performance results are in red and the predicted results are in green. On the X-axis each type of measurement is represented. For example, fc1 refers to the first fully-connected layer. On the Y-axis we have the time in seconds. The model is accurate when the green bars resemble the red bars.

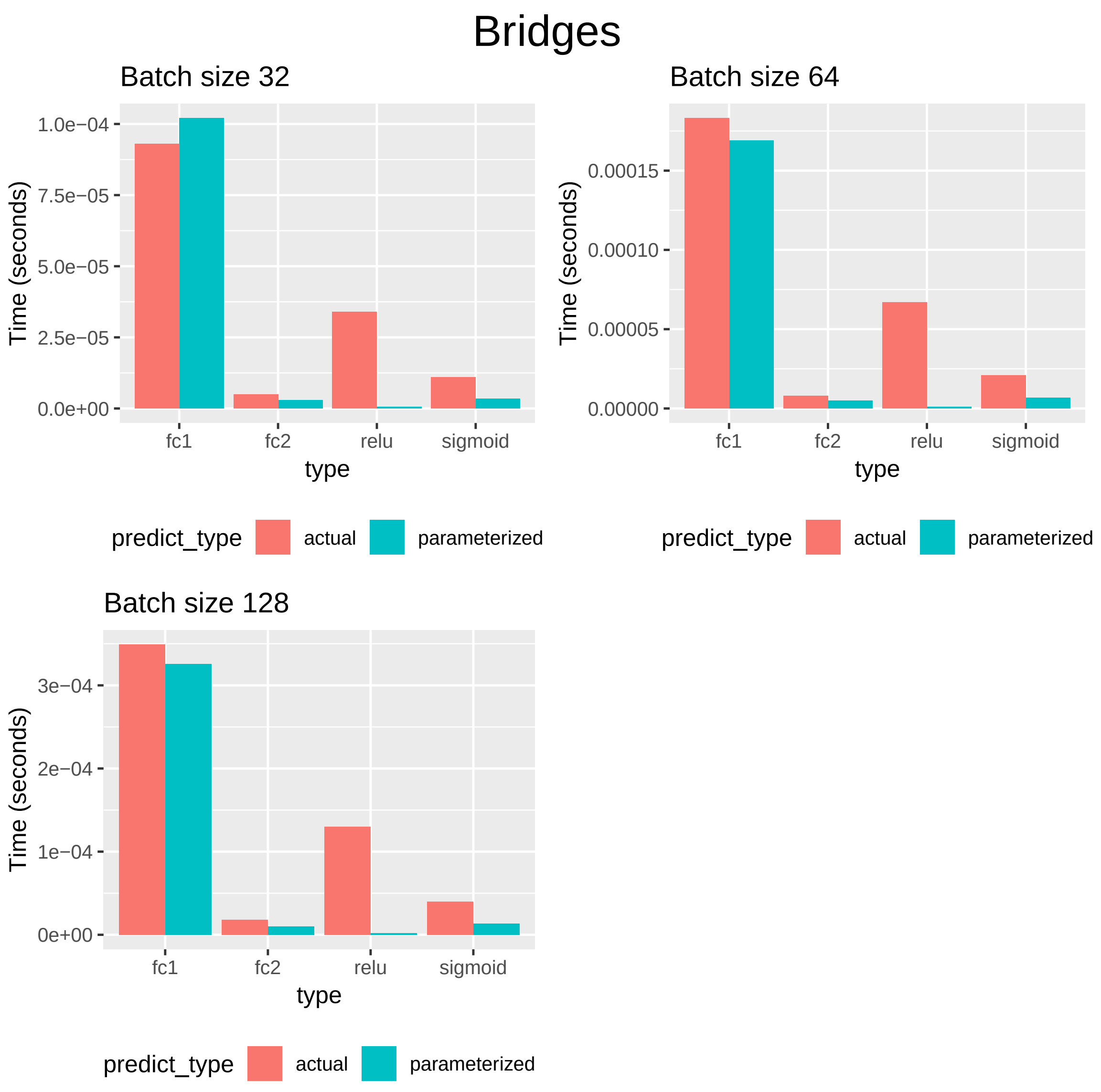

Fig. 3.2. Results for the simple network on Bridges.

Table 3.7.
Results for the simple network on Bridges.

Type	Batch Size	Actual	Predicted	Absolute Percentage Error
fc1	32	0.000093	0.000102	9.68
relu	32	0.000034	0.000001	98.35
fc2	32	0.000005	0.000003	40.00
sigmoid	32	0.000011	0.000003	69.49
fc1	64	0.000183	0.000169	7.65
relu	64	0.000067	0.000001	98.33
fc2	64	0.000008	0.000005	37.50
sigmoid	64	0.000021	0.000007	68.04
fc1	128	0.000349	0.000326	6.59
relu	128	0.000130	0.000002	98.28
fc2	128	0.000018	0.000010	44.44
sigmoid	128	0.000040	0.000013	66.44

Table 3.8.
A summary of the results using MAPE.

System	Batch Size	Mean Absolute Percentage Error
Carbonate	32	61.96
Carbonate	64	57.89
Carbonate	128	44.36
Bridges	32	54.38
Bridges	64	52.88
Bridges	128	53.94

4. SUMMARY

We have proposed two performance models in this thesis. For the first, we extended the Roofline model to handle network communication. This involved adding the concept of communication arithmetic intensity to the model while retaining the efficacy of the original model with regard to memory performance. For the second, we created a parameterized model for deep neural networks. This involved measuring performance results on the target systems and using them to predict performance using the problem size. We evaluated both methods of performance prediction on relevant applications and computer platforms.

REFERENCES

[1] S. Williams, A. Waterman, and D. Patterson, “Roofline: an insightful visual performance model for multicore architectures,” *Communications of the ACM*, vol. 52, no. 4, pp. 65–76, Apr. 2009.

[2] K. Kim, K. Kim, and Q. Park, “Performance analysis and optimization of three-dimensional FDTD on GPU using roofline model,” *Computer Physics Communications*, vol. 182, no. 6, pp. 1201–1207, Jun. 2011.

[3] J. W. Choi, D. Bedard, R. Fowler, and R. Vuduc, “A roofline model of energy,” in *2013 IEEE 27th International Symposium on Parallel and Distributed Processing.* IEEE, May 2013.

[4] D. Rossinelli, C. Conti, and P. Koumoutsakos, “Mesh-particle interpolations on graphics processing units and multicore central processing units,” *Philosophical Transactions of the Royal Society A: Mathematical, Physical and Engineering Sciences*, vol. 369, no. 1944, pp. 2164–2175, May 2011.

[5] D. Marques, H. Duarte, A. Ilic, L. Sousa, R. Belenov, P. Thierry, and Z. A. Matveev, “Performance analysis with cache-aware roofline model in Intel advisor,” in *2017 International Conference on High Performance Computing & Simulation (HPCS).* IEEE, Jul. 2017.

[6] A. Bhatelé, L. Wesolowski, E. Bohm, E. Solomonik, and L. V. Kalé, “Understanding application performance via micro-benchmarks on three large supercomputers: Intrepid, ranger and jaguar,” *The International Journal of High Performance Computing Applications*, vol. 24, no. 4, pp. 411–427, May 2010.

[7] T. Kielmann, H. E. Bal, and K. Verstoep, “Fast measurement of logp parameters for message passing platforms,” in *Proceedings of the 15 IPDPS 2000 Workshops on Parallel and Distributed Processing*, ser. IPDPS ’00. London, UK, UK: Springer-Verlag, 2000, pp. 1176–1183.

[8] K. Asanovic, J. Wawrzynek, D. Wessel, K. Yelick, R. Bodik, J. Demmel, T. Keaveny, K. Keutzer, J. Kubiatowicz, N. Morgan, D. Patterson, and K. Sen, “A view of the parallel computing landscape,” *Communications of the ACM*, vol. 52, no. 10, p. 56, Oct. 2009.

[9] J. J. Dongarra, J. D. Cruz, S. Hammerling, and I. S. Duff, “A set of level 3 basic linear algebra subprograms,” *ACM Transactions on Mathematical Software (TOMS)*, vol. 16, no. 1, pp. 1–17, Mar. 1990.

[10] J. D. McCalpin, “Memory bandwidth and machine balance in current high performance computers,” *IEEE Computer Society Technical Committee on Computer Architecture (TCCA) Newsletter*, pp. 19–25, Dec. 1995.

[11] G. Ofenbeck, R. Steinmann, V. Caparros, D. G. Spampinato, and M. Puschel, "Applying the roofline model," in *2014 IEEE International Symposium on Performance Analysis of Systems and Software (ISPASS)*, Mar. 2014, pp. 76–85.

[12] R. Thakur and W. D. Gropp, "Improving the performance of collective operations in MPICH," in *Recent Advances in Parallel Virtual Machine and Message Passing Interface*. Springer Berlin Heidelberg, 2003, pp. 257–267.

[13] C. Nugteren and H. Corporaal, "The boat hull model: Adapting the roofline model to enable performance prediction for parallel computing," in *Proceedings of the 17th ACM SIGPLAN Symposium on Principles and Practice of Parallel Programming*, ser. PPoPP '12. New York, NY, USA: ACM, 2012, pp. 291–292.

[14] A. Ilic, F. Pratas, and L. Sousa, "Cache-aware roofline model: Upgrading the loft," *IEEE Computer Architecture Letters*, vol. 13, no. 1, pp. 21–24, Jan. 2014.

[15] S. J. Cho, S. H. Yun, and J. W. Jeon, "A roofline model based on working set size for embedded systems," *IEICE Electronics Express*, vol. 11, no. 15, 2014.

[16] N. Denoyelle, B. Goglin, A. Ilic, E. Jeannot, and L. Sousa, "Modeling large compute nodes with heterogeneous memories with cache-aware roofline model," in *Lecture Notes in Computer Science*. Springer International Publishing, Dec. 2017, pp. 91–113.

[17] V. C. Cabezas and M. Puschel, "Extending the roofline model: Bottleneck analysis with microarchitectural constraints," in *2014 IEEE International Symposium on Workload Characterization (IISWC)*. IEEE, Oct. 2014.

[18] O. G. Lorenzo, T. F. Pena, J. C. Cabaleiro, J. C. Pichel, and F. F. Rivera, "3DyRM: a dynamic roofline model including memory latency information," *The Journal of Supercomputing*, vol. 70, no. 2, pp. 696–708, Mar. 2014.

[19] J. D. Suetterlein, J. Landwehr, A. Marquez, J. Manzano, and G. R. Gao, "Extending the roofline model for asynchronous many-task runtimes," in *2016 IEEE International Conference on Cluster Computing (CLUSTER)*. IEEE, Sep. 2016.

[20] S. Fortune and J. Wyllie, "Parallelism in random access machines," in *Proceedings of the Tenth Annual ACM Symposium on Theory of Computing*, ser. STOC '78. New York, NY, USA: ACM, 1978, pp. 114–118.

[21] L. G. Valiant, "A bridging model for parallel computation," *Commun. ACM*, vol. 33, no. 8, pp. 103–111, Aug. 1990.

[22] R. H. Bisseling and W. F. McColl, "Scientific computing on bulk synchronous parallel architectures," in *Technology and Foundations - Information Processing '94, Volume 1, Proceedings of the IFIP 13th World Computer Congress, Hamburg, Germany, 28 August - 2 September, 1994*, 1994, pp. 509–514.

[23] D. Culler, R. Karp, D. Patterson, A. Sahay, K. E. Schauser, E. Santos, R. Subramonian, and T. von Eicken, "LogP: towards a realistic model of parallel computation," in *Proceedings of the fourth ACM SIGPLAN symposium on Principles and practice of parallel programming - PPOPP 93*. ACM Press, 1993.

[24] A. Alexandrov, M. F. Ionescu, K. E. Schauser, and C. Scheiman, "LogGP," in *Proceedings of the seventh annual ACM symposium on Parallel algorithms and architectures - SPAA 95*. ACM Press, 1995.

[25] M. Frigo, C. E. Leiserson, H. Prokop, and S. Ramachandran, "Cache-oblivious algorithms," in *Proceedings of the 40th Annual Symposium on Foundations of Computer Science*, ser. FOCS '99. Washington, DC, USA: IEEE Computer Society, 1999, pp. 285–298.

[26] A. Pedram, J. D. Mccalpin, and A. Gerstlauer, "A highly efficient multicore floating-point fft architecture based on hybrid linear algebra/fft cores," *J. Signal Process. Syst.*, vol. 77, no. 1-2, pp. 169–190, Oct. 2014.

[27] S. Williams. (2018) Roofline performance model. Lawrence Berkeley National Laboratory. Accessed Nov. 25, 2018. [Online]. Available: https://crd.lbl.gov/departments/computer-science/PAR/research/roofline/

[28] L. Allulli, "Cache oblivious computation of shortest paths: Theoretical and practical issues," 2007.

[29] G. S. Brodal, "Cache-oblivious algorithms and data structures," in *Algorithm Theory - SWAT 2004, 9th Scandinavian Workshop on Algorithm Theory, Humlebaek, Denmark, July 8-10, 2004, Proceedings*, 2004, pp. 3–13.

[30] R. A. V. D. Geijn and J. Watts, "SUMMA: scalable universal matrix multiplication algorithm," *Concurrency: Practice and Experience*, vol. 9, no. 4, pp. 255–274, Apr. 1997.

[31] P. Jähne, "Erzeugung minimaler spannbäume auf ungerichteten, kantengewichteten graphen mit den algorithmen von kruskal, prim und boruvka," in *45. Jahrestagung der Gesellschaft für Informatik, Informatik 2015, Informatik, Energie und Umwelt, 28. September - 2. Oktober 2015 in Cottbus, Deutschland*, 2015, pp. 1937–1947.

[32] A. de Myttenaere, B. Golden, B. L. Grand, and F. Rossi, "Mean absolute percentage error for regression models," *Neurocomputing*, vol. 192, pp. 38–48, Jun. 2016.

[33] A. Calotoiu, D. Beckingsale, C. W. Earl, T. Hoefler, I. Karlin, M. Schulz, and F. Wolf, "Fast multi-parameter performance modeling," in *2016 IEEE International Conference on Cluster Computing, CLUSTER 2016, Taipei, Taiwan, September 12-16, 2016*, 2016, pp. 172–181.

[34] D. Zaparanuks and M. Hauswirth, "Algorithmic profiling," *SIGPLAN Not.*, vol. 47, no. 6, pp. 67–76, Jun. 2012. [Online]. Available: http://doi.acm.org/10.1145/2345156.2254074

[35] F. Yan, O. Ruwase, Y. He, and T. Chilimbi, "Performance modeling and scalability optimization of distributed deep learning systems," in *Proceedings of the 21th ACM SIGKDD International Conference on Knowledge Discovery and Data Mining*, ser. KDD '15. New York, NY, USA: ACM, 2015, pp. 1355–1364. [Online]. Available: http://doi.acm.org/10.1145/2783258.2783270

[36] Z. Pei, C. Li, X. Qin, X. Chen, and G. Wei, "Iteration time prediction for CNN in multi-gpu platform: Modeling and analysis," *IEEE Access*, vol. 7, pp. 64 788–64 797, 2019. [Online]. Available: https://doi.org/10.1109/ACCESS.2019.2916550

[37] N. A. Nystrom, M. J. Levine, R. Z. Roskies, and J. R. Scott, “Bridges: A uniquely flexible hpc resource for new communities and data analytics,” in *Proceedings of the 2015 XSEDE Conference: Scientific Advancements Enabled by Enhanced Cyberinfrastructure*, ser. XSEDE ’15. New York, NY, USA: ACM, 2015, pp. 30:1–30:8. [Online]. Available: http://doi.acm.org/10.1145/2792745.2792775